

**EFFECT OF OXYGEN-CONTAINING FUNCTIONAL GROUPS ON
METHANE ADSORPTION BY ACTIVATED CARBON**

Kittima Dheerapreampree

A Thesis Submitted in Partial Fulfilment of the Requirements
for the Degree of Master of Science
The Petroleum and Petrochemical College, Chulalongkorn University
in Academic Partnership with
The University of Michigan, The University of Oklahoma,
Case Western Reserve University, and Institut Français du Pétrole
2017

บทคัดย่อและแฟ้มข้อมูลฉบับเต็มของวิทยานิพนธ์ตั้งแต่ปีการศึกษา 2554 ที่ให้บริการในคลังปัญญาจุฬาฯ (CUIR)
เป็นแฟ้มข้อมูลของนิสิตเจ้าของวิทยานิพนธ์ที่ส่งผ่านทางบัณฑิตวิทยาลัย

The abstract and full text of theses from the academic year 2011 in Chulalongkorn University Intellectual Repository (CUIR)
are the thesis authors' files submitted through the Graduate School.

ABSTRACT

5673011063: Petroleum Technology Program

Kittima Dheerapreampree: Effect of Oxygen-Containing Functional Groups on Methane Adsorption by Activated Carbon.

Thesis Advisors: Assoc. Prof. Boonyarach Kitiyanan, Prof. Pramoch Rangsunvigit 63 pp.

Keywords: Activated carbon/ Adsorption/ Methane/ Oxygen-Containing Functional Groups

Natural gas has been applied as a fuel for vehicle because it is cheaper and cleaner burning than other fuels. In the vehicle, natural gas is ordinarily reserved by compressing and storing under high pressure at room temperature but this method has several limitations (e.g. low energy density, high weight of tank). Therefore, a porous material with high specific surface area (e.g. activated carbon) is suggested to eliminate the limitations of natural gas storage by compression, natural gas is adsorbed at relatively low pressure and room temperature. The adsorption capacity of activated carbons is related with their physical and chemical surface properties. In this study, bituminous activated carbon was modified by different methods to produce different quantity of oxygen-containing functional groups on activated carbon surface (1) by acid solution or (2) by alkali solution, for studying the relation between oxygen-containing functional groups and the adsorption capacity of methane on activated carbon surface. The physical properties of the activated carbon were elucidated by using Brunauer-Emmett-Teller (BET) surface analysis. Boehm titration technique and Fourier Transform Infrared Spectroscopy (FTIR) were applied for qualitative and quantitative analyses of oxygen-containing functional groups. The results confirmed the presence of oxygen-containing functional groups on the activated carbon surface consisting of phenolic group, lactone group and carboxylic group. The oxygen-containing functional groups on the surface of activated carbon play an important role on the methane adsorption but the methane adsorption also depends on other surface properties of activated carbon.

บทคัดย่อ

กฤติมา อีระเปรมปรี : ผลของหมู่ฟังก์ชันออกซิเจนต่อการการดูดซับมีเทนด้วยถ่านกัมมันต์ (Effect of Oxygen-Containing Functional Groups on Methane Adsorption by Activated Carbon) อ. ที่ปรึกษา : รศ. ดร. บุญยรัชต์ กิตยานันท์ และ ศ. ดร. ปราโมช รังสรรค์วิจิตร 63 หน้า

ก๊าซธรรมชาติถูกใช้เป็นเชื้อเพลิงสำหรับยานพาหนะเนื่องจากมีราคาถูกและมีการเผาไหม้ที่สะอาดกว่าเชื้อเพลิงชนิดอื่น ในยานพาหนะแก๊สธรรมชาติมักถูกกักเก็บโดยวิธีการอัดและกักเก็บภายใต้แรงดันสูงที่อุณหภูมิห้อง แต่วิธีนี้ยังมีข้อจำกัดหลายอย่าง (เช่น ความหนาแน่นพลังงานต่ำ น้ำหนักถังมาก) ดังนั้นจึงมีการสนใจวัสดุที่มีรูพรุน ซึ่งมีพื้นที่ผิวจำเพาะมาก (เช่น ถ่านกัมมันต์) มาใช้เพื่อแก้ไขข้อจำกัดของการกักเก็บด้วยการบีบอัด โดยวิธีการนี้ ก๊าซธรรมชาติจะถูกกักเก็บที่ความดันต่ำและอุณหภูมิห้อง ซึ่งความสามารถในการดูดซับของถ่านกัมมันต์จะขึ้นอยู่กับคุณสมบัติทางกายภาพและคุณสมบัติทางเคมี ในการศึกษานี้ได้นำถ่านกัมมันต์จากถ่านหินบิทูมินัสไปผ่านการปรับสภาพด้วยตัวปรับสภาพที่แตกต่างกัน เพื่อให้ได้ปริมาณที่แตกต่างกันของหมู่ฟังก์ชันออกซิเจน 1) ปรับสภาพโดยสารละลายกรด 2) ปรับสภาพโดยสารละลายอัลคาไล เพื่อที่จะศึกษาความสัมพันธ์ระหว่างหมู่ฟังก์ชันออกซิเจนกับการดูดซับก๊าซมีเทน ถ่านกัมมันต์จะถูกนำไปตรวจลักษณะทางกายภาพด้วยเครื่องมือการวิเคราะห์พื้นที่ผิวและวิเคราะห์ชนิดและปริมาณของหมู่ฟังก์ชันโดยการผ่านแสงอินฟราเรดและการไทเทรตด้วยวิธีของ Boehm ผลการทดลองยืนยันว่ามีหมู่ฟังก์ชันออกซิเจนบนผิวของถ่านกัมมันต์ประกอบด้วยหมู่ฟีนอลิก หมู่แลคโตน และหมู่คาร์บอกซิลิก หมู่ฟังก์ชันออกซิเจนบนผิวของถ่านกัมมันต์มีผลต่อการดูดซับมีเทนแต่การดูดซับมีเทนก็ยังขึ้นอยู่กับคุณสมบัติพื้นผิวของถ่านกัมมันต์อีกด้วย

ACKNOWLEDGEMENTS

First of all, I would like to express my deep appreciation to my advisors, Assoc. Prof. Boonyarach Kitiyanan, and Prof. Pramoch Rangsunvigit for their valuable recommendation, encouragement, and understanding throughout this thesis work. Their positive attitudes contributed significantly to inspire and maintain my enthusiasm throughout the whole period.

I would like to sincerely thank Prof. Thirasak Rirksomboon and Assoc. Prof. Vissanu Meeyoo for kindly serving on my thesis committee. Their sincere suggestions are definitely imperative for accomplishing my thesis.

I am grateful for the partial scholarship and partial funding of the thesis work provided by the Petroleum and Petrochemical College, Chulalongkorn University.

My gratitude is also extended to all staffs of the Petroleum and Petrochemical College, Chulalongkorn University, for their kind assistance and cooperation.

I would like to thank all of my PPC friends for their friendly help, creative suggestions, and cheerfulness. I had the enjoyable time working with them all.

Finally, I would like to express my sincere gratitude to my family for their understanding and unconditional support.

TABLE OF CONTENTS

	PAGE
Title page	i
Abstract (in English)	iii
Abstract (in Thai)	iv
Acknowledgements	v
Table of Contents	vi
List of Tables	ix
List of Figures	xi
Abbreviations	xiii

CHAPTER

I	INTRODUCTION	1
II	LITERATURE REVIEW	3
	2.1 Natural Gas	3
	2.2 Natural Gas Storage	4
	2.2.1 Compressed Natural Gas (CNG)	5
	2.2.2 Liquefied Natural Gas (LNG)	5
	2.2.3 Adsorbed Natural Gas (ANG)	6
	2.3 Adsorption	7
	2.4 Adsorption Isotherms	8
	2.4.1 IUPAC Classification of Adsorption Isotherms	9
	2.5 Activated Carbon	11
	2.6 Literature Review	13
	2.6.1 Methane Adsorption by Several Types of Activated Carbon	13
	2.6.2 Effect of Oxygen-Containing Functional Groups on Several Type Adsorbent	16

CHAPTER		PAGE
III	EXPERIMENTAL	22
	3.1 Materials and Equipment	22
	3.1.1 Adsorbents	22
	3.1.2 Gases	22
	3.1.3 Chemicals	22
	3.1.4 Equipment	23
	3.2 Experimental Procedures	23
	3.2.1 Activated Carbon Characterizations	23
	3.2.2 Adsorption Measurement	24
	3.2.3 Activated Carbons Surface Treatment	26
IV	RESULTS AND DISCUSSION	28
	4.1 Activated Carbon Characterizations	28
	4.1.1 Surface Area Analysis of Activated Carbons	28
	4.1.2 Infrared Spectroscopy Characterization of Activated Carbons	29
	4.1.3 Boehm Titration	30
	4.2 Adsorption of Methane on Modified and Un-modified Activated Carbon	32
V	CONCLUSIONS AND RECOMMENDATION	42
	5.1 Conclusions	42
	5.2 Recommendation	42

CHAPTER	PAGE
REFERENCES	43
APPENDICES	47
Appendix A Methane Adsorption on Each Studied Activated Carbon at 35 °C	47
Appendix B Ash Content of Activated Carbon	61
Appendix C The Relationship Between Methane Adsorption Capacity and BET Surface Area from Previous Studies	62
CURRICULUM VITAE	63

LIST OF TABLES

TABLE	PAGE	
2.1	Typical composition of natural gas	3
2.2	Interaction and porosity of adsorption isotherms for six types	9
4.1	BET surface area, micropore volume, total pore volume and average micropore diameter of studied activated carbons	28
4.2	Quantification of oxygen-containing functional groups by Boehm titration	31
4.3	Methane adsorption capacity (mmol/g) of adsorbents at 900 psi and 35 °C	34
4.4	Methane adsorption capacity ($\mu\text{mol}/\text{m}^2$) of adsorbent at 900 psi and 35 °C	38
A1	The amount of methane adsorption (mmol/g) on AC/Untreated	47
A2	The amount of methane adsorption ($\mu\text{mol}/\text{m}^2$) on AC/Untreated	48
A3	The amount of methane adsorption (mmol/m^2) on AC/De-ash	49
A4	The amount of methane adsorption ($\mu\text{mol}/\text{m}^2$) on AC/De-ash	50
A5	The amount of methane adsorption (mmol/m^2) on AC/NaOH	51
A6	The amount of methane adsorption ($\mu\text{mol}/\text{m}^2$) on AC/NaOH	52
A7	The amount of methane adsorption (mmol/m^2) on AC/KOH	53
A8	The amount of methane adsorption ($\mu\text{mol}/\text{m}^2$) on AC/KOH	54
A9	The amount of methane adsorption (mmol/m^2) on AC/ $\text{NH}_3 \cdot \text{H}_2\text{O}$	55

TABLE		PAGE
A10	The amount of methane adsorption ($\mu\text{mol}/\text{m}^2$) on AC/ $\text{NH}_3 \cdot \text{H}_2\text{O}$	56
A11	The amount of methane adsorption (mmol/m^2) on AC/ H_2SO_4	57
A12	The amount of methane adsorption ($\mu\text{mol}/\text{m}^2$) on AC/ H_2SO_4	58
A13	The amount of methane adsorption (mmol/m^2) on AC/ H_2O_2	59
A14	The amount of methane adsorption ($\mu\text{mol}/\text{m}^2$) on AC/ H_2O_2	60
B1	Ash content of activated carbon	61

LIST OF FIGURES

FIGURE	PAGE
2.1 CNG and ANG storage tank.	6
2.2 Comparison of the methane adsorption capacity of CNG and ANG storage.	7
2.3 The IUPAC classification for adsorption isotherms.	11
2.4 The pores structure of activated carbon.	12
2.5 Methane stored of various activated carbon compare with compressed gas storage.	16
2.6 Surface functional groups of various activated carbon (mmol/g).	18
3.1 Schematic of the volumetric apparatus.	24
4.1 FTIR spectra of the treated and untreated activated carbons.	30
4.2 Specific amount of oxygen-containing functional groups on surface of activated carbon samples.	32
4.3 Methane adsorption capacity (mmol/g) on activated carbon samples at 35 °C.	33
4.4 Methane adsorption capacity (mmol/g) at 900 psia and 35 °C as a function of micropore volume (cm ³ /g).	34
4.5 Methane adsorption capacity (mmol/g) at 900 psia and 35 °C as a function of total pore volume (cm ³ /g).	35
4.6 Methane adsorption capacity (mmol/g) at 900 psia and 35 °C as a function of Average micropore diameter (Å).	35
4.7 Methane adsorption capacity (mmole/g) at 900 psia and 35 °C as a function of BET surface area (m ² /g).	36
4.8 Methane adsorption capacity (μmol/m ²) on activated carbons samples at 35 °C.	37
4.9 Methane adsorption capacity (μmol/m ²) at 900 psia and 35 °C as a function of carboxylic group (mmol/g).	38

FIGURE		PAGE
4.10	Methane adsorption capacity ($\mu\text{mol}/\text{m}^2$) at 900 psia and 35 °C as a function of latone group (mmol/g).	39
4.11	Methane adsorption capacity ($\mu\text{mol}/\text{m}^2$) at 900 psia and 35 °C as a function of phenolic group (mmol/g).	39
4.12	Methane adsorption capacity ($\mu\text{mol}/\text{m}^2$) at 900 psia and 35 °C as a function of total oxygen containing group (mmol/g).	41
C 1	Methane adsorption capacity (mmol/g) at 1000 psia and 40 °C as a function of BET surface area (m^2/g).	62
C 2	Methane adsorption capacity (mmol/g) at 900 psia and 35 °C as a function of BET surface area (m^2/g).	62

ABBREVIATIONS

AC/Untreated	Untreated bituminous coal-based activated carbon
AC/De-ash	Deashed bituminous coal-based activated carbon
AC/NaOH	Bituminous coal-based activated carbon treated by NaOH
AC/KOH	Bituminous coal-based activated carbon treated by KOH
AC/NH ₃ ·H ₂ O	Bituminous coal-based activated carbon treated by NH ₃ ·H ₂ O
AC/H ₂ SO ₄	Bituminous coal-based activated carbon treated by H ₂ SO ₄
AC/H ₂ O ₂	Bituminous coal-based activated carbon treated by H ₂ O ₂

CHAPTER I

INTRODUCTION

Natural gas (NG) has been utilized as a fuel for vehicle because it is cheaper and cleaner burning than other fossil fuels. Natural gas is composed mainly of methane which is the highest H/C ratio in its molecule and has a higher octane number than typical gasoline.

However, methane has major disadvantage, methane is a gas at STP and has low energy density only 0.038 MJ/L (0.11% of gasoline). The potential technological options to increase the energy density for natural gas are three different methods storages, liquefied natural gas (LNG), compressed natural gas (CNG) and adsorbed natural Gas (ANG). LNG is stored in a cryogenic tank as a boiling point liquid about 112K (-162 °C) at 0.1MPa, that energy density is 23 MJ/L (66% of gasoline). LNG is not suitable for vehicles because it requires a special tank to stabilize the very low temperature. CNG is usually used for natural gas storage for vehicle by compressing natural gas and storing under high pressure (higher than 3,000 psi at ambient temperature) The energy density of CNG is about 8.8 MJ/L (25% of gasoline). CNG requires high pressure therefore the storage tank must be very thick and strong steel causing the higher weight to the vehicles. To eliminate the limitations of NG storage in vehicles, ANG is a technology in which natural gas is adsorbed by a porous material such as zeolites, carbon nanotubes and activated carbon at relatively low pressure and room temperature (Lozano-Castelló *et al.*, 2002).

Activated carbon as a methane adsorbent offers several benefits, due to its high porosity and high specific surface area. The adsorption capacity of activated carbons is related to their physical and chemical surface properties. The types of heteroatoms can influence on surface characteristics of activated carbon, for example oxygen atom (Derylo-Marczewska *et al.*, 2011). Removing oxygen groups can possibly improve adsorption capacity of hydrophobic volatile organic compounds (VOCs) on activated carbon (Li *et al.*, 2011).

This research studies the relation between oxygen-containing functional groups on surface of activated carbon and the methane adsorption by activated carbon.

The activated carbon is modified either (1) by acid solution H_2O_2 and H_2SO_4 or (2) by alkali solution NaOH , KOH and $\text{NH}_3\text{H}_2\text{O}$. The adsorption capacity of methane on activated carbon samples are investigated by volumetric apparatus under the pressure up to 1000 psia at 35°C . The physical properties of the activated carbon are defined by Brunauer-Emmett-Teller (BET) surface analysis. Boehm titration technique and Fourier Transform Infrared Spectrophotometer (FTIR) are applied for qualitative and quantitative oxygen-containing functional groups on activated carbon samples.

CHAPTER II

LITERATURE REVIEW

2.1 Natural Gas

Natural gas is a fossil fuel, trapped in the underground and usually found in association with petroleum deposit. Same as the other fossil fuel, natural gas is originated from the decomposition of plant or animal remains at very high pressure and high temperatures for a very long time. Table 2.1 shows the typical composition of natural gas before it is refined, which consisting mainly of methane followed by ethane, propane, butane, CO₂, N₂, and other trace gases.

Table 2.1 Typical composition of natural gas (Boehm and Saba, 2009)

Constituent	Chemical Formula	Composition (mol%)
Methane	CH ₄	60-90
Ethane	C ₂ H ₆	0-20
Propane	C ₃ H ₈	
Butane	C ₄ H ₁₀	
Carbon Dioxide	CO ₂	0-8
Oxygen	O ₂	0-0.2
Nitrogen	N ₂	0-5
Hydrogen sulphide	H ₂ S	0-5
Rare gases	A, He	0-2

After extraction from the wells, natural gas is refined to remove impurities when it is almost pure methane. Methane is colorless, odorless, non-carcinogenic and non-toxic gas. Thus, it is filled up with mercaptan, which is an odorant for aids in detecting any leaks. A methane molecule consists of one carbon atom and four hydrogen atoms. CH₄ is its formula.

The combustion of methane is an exothermic reaction, shown as chemical equation 2.1. One molecule of methane is reacting with two molecules of oxygen, which in gaseous form and produce one molecule of carbon dioxide in gaseous form, two molecules of water in liquid form and the energy released from the reaction is - 891 kJ.



Compared with other petroleum fuels, natural gas is an environmentally friendly one, it is cleaner burning and emits lower pollution into the air include 25% less carbon dioxide emissions and 60-90% less smog-forming volatile organic compounds when compared to diesel (Lozano-Castelló *et al.*, 2002).

Nowadays, natural gas used as a fuel for the vehicle is rapidly increasing because it offers many environmental benefits and cheaper than gasoline and diesel. However, it has important drawback of using natural gas in vehicles. Natural gas has lower energy density than conventional and other alternative fuels at ambient conditions, which causes the driving range of natural gas based-fuel less than conventional and other alternative fuels. Therefore, it requires a higher capacity of the natural gas than the others fuel to driving in the same distance. According to the limitation of the car space, a storage technology requires a higher energy density. Then, the possible technological options are compression natural gas (CNG), liquefied natural gas (LNG) and adsorbed natural gas (ANG).

2.2 Natural Gas Storage

For using natural gas, natural gas storage one of the barriers to be safe and effective. Since natural gas composes mainly of methane, which is a small molecule, it is hard to store in a high density. Researchers have developed the option to carry higher capacity of natural gas for transportation. The following are the way to store natural gas.

2.2.1 Compressed Natural Gas (CNG)

CNG is broadly method for fixable the low energy density of natural gas by compressing it to a pressure of 200 to 250 bars and storing on-board the vehicle in the pressure cylinders. The natural gas cylinder is usually produced from steel that variety of volumes and dimensions depend on the different type of vehicles, because of high pressure in the tank it requires specially-designed such as multi-layer wrapping, which is heavy weight and requires a lot of space. Moreover, the CNG cylinder needs to refueling up more often than the gasoline or diesel tank.

CNG cylinders normally sit in the boot of a car, in the cargo area of a light goods vehicle (LGV), in the chassis structure of a truck and on the rooftop or under the floor of a bus. The cylinders are connected to a refueling point, which may be under the bonnet or on the vehicle body. A standard connector is used to allow a vehicle to refuel at any CNG station. Two sizes of the connector are used, a smaller type for cars and LGVs and high flow type for trucks and buses to refuel in the lowest time. CNG at storage pressure is piped from the cylinder to a point close to the engine, where a regulator reduces the pressure to a level suitable for the control system which feeds gas to the intake manifold. This control device may be a mechanical pressure governor or electronic control system designed for use with an engine management to control vehicle emissions (Hassan Eftekhari *et al.*, 2009).

2.2.2 Liquefied Natural Gas (LNG)

In this method, natural gas is liquefied under pressure of 10-20 bar at the boiling point $-161.5\text{ }^{\circ}\text{C}$ and stored as a liquid in a cryogenic tank or composite vessel. The shape of LNG storage tanks classically is a cylinder or spherical (Solar *et al.*, 2010). LPG fed to the engine is controlled by a regulator or vaporizer, which converts the LPG to a vapor. The vapor is fed to a mixer located near the intake manifold, where it is metered and mixed with filtered air before being drawn into the combustion chamber where it is burned to produce power, just like gasoline. LNG requires the use of complex and expensive liquefaction equipment and the refueling infrastructure costs even more than CNG.

2.2.3 Adsorbed Natural Gas (ANG)

ANG is an alternative method of natural gas storage that can store natural gas at considerably higher volumetric capacity than pressurized storage for an equivalent condition by use of adsorption of the gas on an adsorption agent or adsorbent which could be low-cost activated carbon material and molecular sieve in the cylinder. This option can be workable that overcomes the problems about high pressure and low energy density of CNG. Natural gas can be stored as an adsorbed phase in microporous materials at relatively low pressure (7-40 bar) at room temperature. The highest gas storage density becomes the definitive requirement, in order to store and deliver the high volume of gas per volume of storage vessel (v/v). Depending on the adsorption agent characteristics, the volumetric adsorption capacity and delivery would be different as well as the volumetric energy density (Namvar-Asl *et al.*, 2008). ANG technology allows storing large amounts of natural gas in a relatively thin-walled tank filled with adsorbent and refueling the tank using simple and cheap equipment or sometimes refueling directly from natural gas pipelines. Figure 2.1 shows the difference between CNG and ANG storage. In ANG tank, methane molecules adsorbed on the activated carbon adsorbent in micropore structures. Micropore structure is important for methane storage because it gives the highest capacity of adsorbed methane.

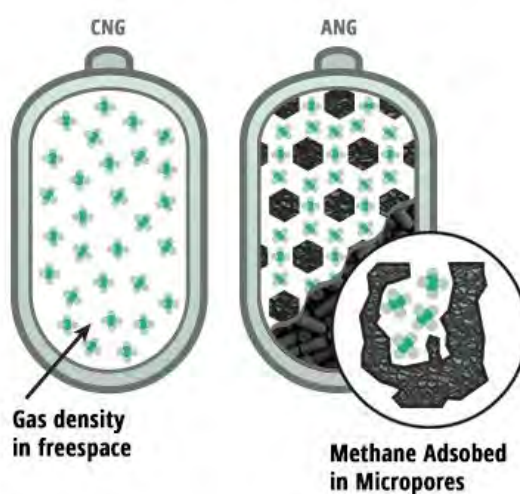


Figure 2.1 CNG and ANG storage tank (www.carboncenter.ru).

The addition of an adsorption agent into the tank, such as activated carbon, makes it possible two things: (i) store a larger volume of natural gas in the same container at the same pressure or (ii) store the same volume of natural gas in the container at a lower pressure, that shows in Figure 2.2. Since activated carbon has a very large surface area because of its porous nature, it gives the ability to adsorb large quantities of natural gas.

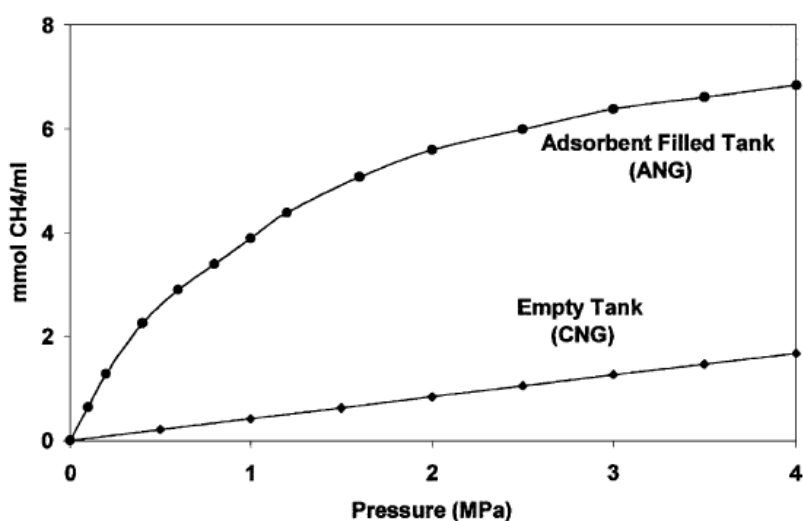


Figure 2.2 Comparison of the methane adsorption capacity of CNG and ANG storage. (Lozano-Castelló *et al.*, 2002).

2.3 Adsorption

Adsorption is present in many natural physical, biological, and chemical systems. It is widely used in industrial applications such as gas separation, transportation, and storage. Adsorption can take place at any solid – fluid interface, gas – solid interface and liquid – solid interface. Adsorption process creates a film of the adsorbate (the molecules or atoms being adsorbed) on the surface of the adsorbent. It is different from absorption process by which the fluid molecules or atoms are diffused into a liquid or solid to form a solution. The term “sorption” includes both adsorption and absorption process, while “desorption” is the reverse of adsorption

Adsorption at the solid-gas interface can be generally classified as physisorption and chemisorption. Physical adsorption or physisorption is reversible adsorption by weak interaction based on the Van der Waals, dipole-dipole or London forces interactions between the adsorbed molecules and between the adsorbate and the substrate; no covalent bonds between the adsorbent and the adsorbate. The enthalpy of physical adsorption is less than 15-20 kJ/mol. Physisorption is a reversible process. Physisorption occurs mostly at low temperatures and occurs as a preliminary stage to chemisorption. Chemisorption is adsorption involving stronger interaction between adsorbate and adsorbent, The formation of a chemical (often covalent) linkage. Heats of chemisorptions are approximately 200 kJ/mol. Chemisorption is almost always exothermic and usually an irreversible process.

2.4 Adsorption Isotherms

Adsorption isotherms are determined of adsorbate quantity on the adsorbent as a function of its pressure (if gas) or concentration (if liquid) at the constant temperature. The amount of adsorption is nearly always normalized by the mass (or specific surface area) of the adsorbent depend on the different materials. Many different types of isotherm can be observed by their characteristic, which depends on types of adsorbate, types of adsorbent and intermolecular interactions between the gas and the surface. When a gas contacts with a solid surface, molecules of the gas will adsorb to the surface in the amount that is a function of their partial pressure in the solid. The measurement of the amount of adsorbed gas over a range of partial pressures at a single temperature in a graph known as an adsorption isotherm. Adsorption isotherm in physical chemistry is commonly expressed as the concentration of adsorbed phase (or amount of gas adsorbed) per unit mass of adsorbent. It is a function of both pressure and temperature, besides the nature of the gas. Isotherms are the closest one to direct experiments, measurements of pure component isotherms easily to be conducted and are available for adsorption design study. concurrently, the investigation of multi-component isotherms often hit a difficulty since the experimental data over design ranges of pressure, temperature, and composition are impractically measurable (Jeong *et al.*, 2007).

2.4.1 IUPAC Classification of Adsorption Isotherms

The adsorption isotherms can have different types according to the type of adsorbent, the type of adsorbate, and intermolecular interactions between the gas and the solid surface. In 1940, the first systematic interpreting adsorption isotherm for gas-solid equilibria was introduced by Brunauer, Deming, Deming, and Teller well known as BDDT. They classified isotherms into five types. These BDDT isotherms and additional one introduced much later by Sing in 1982, which completes the IUPAC classification, 1985. In physical adsorption, adsorption isotherms can be classified as one of six types, as shown in Figure 2.6, respectively. The BDDT and IUPAC classification have two deficiencies: they are incomplete and they give the incorrect impression that adsorption isotherms are always monotonic functions of pressure (Soo-Jin and Min-Kang, 2011).

Table 2.2 Interaction and porosity of adsorption isotherms for six types (Soo-Jin and Min-Kang, 2011)

Type	Interaction between sample surface and adsorbate	Porosity
I	Relatively strong	Micropores (< 2 nm)
II	Relatively strong	Macropores (> 50 nm)
III	Weak	Macropores (> 50 nm)
IV	Relatively strong	Mesopores (2-50 nm)
V	Weak	Mesopores, Micropores
VI	Relatively strong	Nonporous

Type I isotherm characterize microporous adsorbents. Microporous solids for this isotherm having relatively small external surfaces such as activated carbons. These isotherms reach a maximum value of adsorption without inflections. This isotherm is limited to the completion of a single monolayer of adsorbate at the adsorbent surface. At the first part of this isotherm having a relative pressure (p/p^0)

from 0 to about 0.05 is an indication for the dimensions of the micropores. The steeper the gradient the narrower the micropores.

Type II isotherm (sigmoid or S-shaped) describes adsorption on non-porous or macroporous adsorbents. This isotherm indicates the beginning of an unlimited multilayer after completion of the monolayer (the region of relative pressure $(p/p_0) > 0.1$ and $p/p_0 > 0.9$) and is found in adsorbents with a wide pore sizes distribution. At point B, a monolayer is completed and the adsorption occurs in successive layers at higher relative pressure.

Type III isotherm that is convex and describes adsorption with weak adsorbate-adsorbent interactions but strong interactions between adsorbate. This isotherm also describes the formation of multilayer and there is no flat region because the monolayer formation is disappeared.

Type IV isotherm is hysteresis loop, which is associated with capillary condensation occurring in mesopores. This isotherm is quite similar to type II at low relative pressure. The point of inflection indicates the completion of monolayer and the beginning of multilayer adsorption.

Type V isotherm represents mesoporous and microporous adsorbents and quite similar to type III but there is a capillary condensation in pores as the same pore size as type IV isotherm.

Finally, type VI isotherm describes stepwise multilayer adsorption on a uniform non-porous surface. Each step depends on the system and the temperature. These adsorption isotherms are for surfaces with an extremely homogeneous structure such as pyrolytic graphite that uses methane and argon as adsorbate but not N_2 .

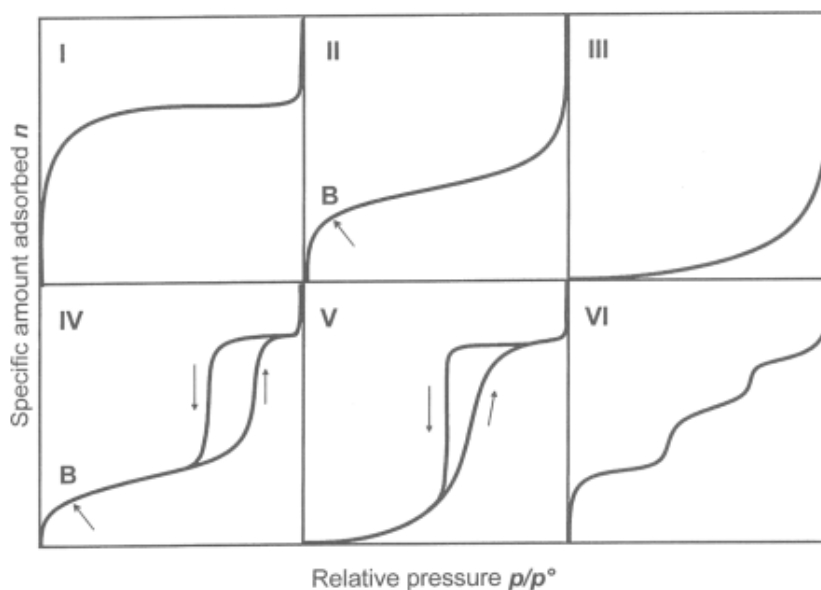


Figure 2.3 The IUPAC classification for adsorption isotherms (Rouquerol *et al.*, 1999).

2.5 Activated Carbon

Activated carbon is a carbonaceous matter, which highly porous and adsorptive. It is widely used for adsorbent because of its benefits such as large specific surface areas, well-developed porosity and tunable surface-containing functional groups (Baker *et al.*, 1992, Zong *et al.*, 2003). For these reasons, activated carbons are generally used as adsorbents for the removal of organic chemicals and metal ions of environmental or economic concern from the air, gases, potable water and wastewater (El-Hendawy *et al.*, 2003). Activated carbons can produced from coconut shell, peat, wood, lignite coal, bituminous coal, olive pits and several carbonaceous materials. The carbon can be produce as powder, granules, pellets, or formed into monoliths or briquettes. Most carbonaceous materials have a porosity and an internal surface area approximately 10-15 m²/g. During the activation process, the internal surface becomes more highly developed and extended by controlled oxidation of carbon atoms. There are two types of activation used in producing activated carbon, which is physical activation and chemical activation. Activated carbon after activation will have an internal surface area approximately between 700 and 1,200 m²/g, depending on the

operating conditions. As a generalization, pore diameters are usually categorized as follows:

Micropores < 40 Angstroms

Mesopores 40-5,000 Angstroms

Macropores > 5,000 Angstroms (typically 5000-20000 Angstroms)

From activation, macropores are primarily formed by the oxidation of weak points (border groups) on the external surface of the raw material. Mesopores are then formed in the walls of the macropores structure. Lastly, the micropores are formed by the planes within the structure of the raw material are attacked by an oxidizing gas. Figure 2.4 shows the macropores, mesopores and micropores structure in an activated carbon.

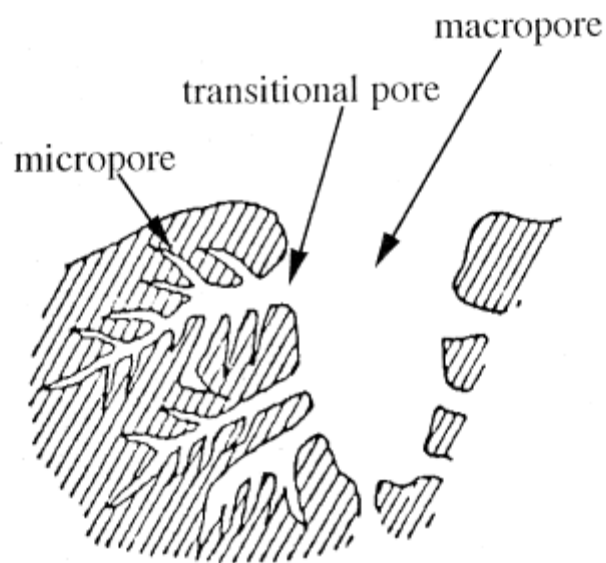


Figure 2.4 The pores structure of activated carbon (Mochida *et al.*, 2000).

Activated carbon also used in the specific industrial applications such as sorption and catalytic industrial, oil and natural gas, food, pharmaceuticals, water treatment, hydro metallurgy, gold recovery and carbon-in-pulp process. Because the activated carbon is produced from naturally occurring raw materials; its properties could be varied.

Compare with other adsorbents, activated carbon plays an important role in the technology of adsorbed natural gas because it adsorbs more nonpolar and weakly polar organic molecules than other adsorbents and it exhibits a low heat of adsorption, resulting in low energy intensive regeneration operations. Interactions between the methane molecules and the surface of carbon increase the density of the adsorbed methane (Rodríguez-Reinoso *et al.*, 2008).

2.6 Literature Review

2.6.1 Methane Adsorption by Several Types of Activated Carbon

Lozano-Castelló *et al.*, (2002) Compared the behaviour of different carbon materials in methane storage. These materials include physically activated carbon fibres (ACFs), chemically activated carbons (ACs) and activated carbon monoliths (ACMs) prepared from different raw materials, different activating agents and different morphologies. The results have been shown that the micropore volume, micropore size distribution (MPSD) of the carbon materials play an important effect in the methane adsorption capacity with direct relationship. Thus, a sample with a higher micropore volume but a much wider MPSD presents a lower methane uptake than a sample with a lower micropore volume but has much optimum pore size for methane adsorption. Moreover, the raw material and activation process method used for its preparation had no effect on adsorption capacity. Also, it showed that methane adsorption capacity depended on the size distribution of micropore.

Balathanigaimani *et al.*, (2006) compared the properties of husk activated carbon and phenol based activated carbon (AC-PH₂O and AC-PKOH) for methane adsorption. To achieve the storage natural gas by using adsorbed natural gas (ANG) was mainly based on the characteristics of the adsorbent. The adsorption experiments were conducted by volumetric method under different constant temperatures (20, 30, 40, and 50°C) and pressure up to 507 psi. The adsorption capacity of methane on activated carbon were defined by using a mass balance equation. The results showed that maximum methane adsorption was observed in AC-RH as its higher surface area than the other adsorbents. The experimental data were

correlated well with Langmuir-Freundlich isotherms because of its flexibility and low percentage error. From Langmuir-Freundlich isotherms indicate that AC-RH has heterogeneous surface while AC-PH₂O and AC-PKOH have homogeneous surfaces. Moreover, isosteric heat of adsorption was calculated by using Clausius-Clapeyron equation. The results from the Clausius-Clapeyron equation also confirmed the Langmuir-Freundlich isotherm results.

Bastos-Neto *et al.* (2007) focused on the effects of textural and surface characteristics of activated carbon on methane adsorption. The textural characteristics were studied by nitrogen adsorption on a surface area analyzer. Elemental and surface analyses were carried out by X-ray photoelectronic spectroscopy (XPS). For the activated carbon from the same raw material, that methane adsorption was related from samples surface area, micropore volume, and narrower pore size distribution within the range of 8–15 Å. There was a common trend for the BET surface area and DR micropore volume to be directly proportional to methane adsorption capacity. Samples with more hydrophobic surfaces had superior methane adsorption properties in comparison to the less hydrophobic samples. Textural parameters were unable to unequivocally determine natural gas storage capacities. Surface chemistry and methane adsorption equilibria were subjects to be considered in the decision-making process when selecting the accurate adsorbent for methane storage.

Najibi *et al.*, (2008) studied the Methane and natural gas storage capacity of three different activated produced from coconut shells, pinewood and lignite with several activating methods. The difference of wet and dry conditions were only add the specific amounts of distilled water with the activated carbon before packing into the cell. This analysis utilized the water proportion ratio (the ratio of the weight of water to the weight of dry activated carbon) at $R_w = 1$. This work was sustained at constant temperature (-196°C) and the pressure was up to 1450 psi. In all types of activated carbons samples, the storage capacity in dry condition methane was higher than in wet conditions natural gas, but the amount of gas delivery was almost the same. Hydrate might occur in the coconut shells based activated carbon at the pressure higher than 4 MPa while the amount of gas stored was less than in dry conditions at overall pressure. The results obtained that the gas released from the activated carbons in each pressure in the dry conditions would change in composition.

Moreover, it also indicated that a number of heavy components were unable to come out of the bed even applied at very low pressures. The higher molecular weight species are more strongly adsorbed than methane, especially in the low-pressure region. These higher molecular weight components will be preferentially adsorbed on activated carbon and therefore the amount of methane that can be delivered by the storage system will decrease.

Bagheri and Abedi (2011) studied the effects of methane adsorption by corn cobs based activated carbon at four different pressures (500, 1000, 1500 and 2000 psi) and two different temperatures (298 K and 323 K) The samples were prepared chemical activation with potassium hydroxide under optimized variables. Six of the samples with different surface areas were chosen for methane adsorption experiments in a volumetric adsorption apparatus. From the methane adsorption capacity showed that adsorption capacity of methane depends on pressure and temperature. When the pressure increases from 500 to 1500 psi, the stored methane capacity increased from 120 (v/v) to 160 (v/v), the maximum increase was about 42%. As temperature increases from 298K to 323 K, the decreases reach about 72%, reducing the stored methane capacity from 120 to 70 (v/v). The highest methane storage capacity was found to be 160 (v/v) at 298K and 1500 psi. The applications include use in the Finally, the result has been presented, corn cobs can be produced a high surface area (900–1300 m²/g) activated carbon with a methane uptake greater than 150 (v/v).

Beckner *et al.*, (2015) studied the properties of five standard high surface area adsorbent for methane storage, one activated carbon (AC), three metal–organic frameworks (MOFs) and one porous polymer (PP) by measuring the potential of these materials to store methane in a 110 L pressure tank at room temperature in term of adsorption and sample density data. At 50 bar, all adsorbent storage definitely stores more than traditional compressed gas storage. Furthermore, an activated carbon and a copper based metal–organic framework (Cu-BTC) showed improvement over compressed gas storage at 250 bar. The driving ranges calculated from storage data demonstration that with an adsorbent, a 110 L tank filled to 50 bar could have a driving range of up to 140 miles.

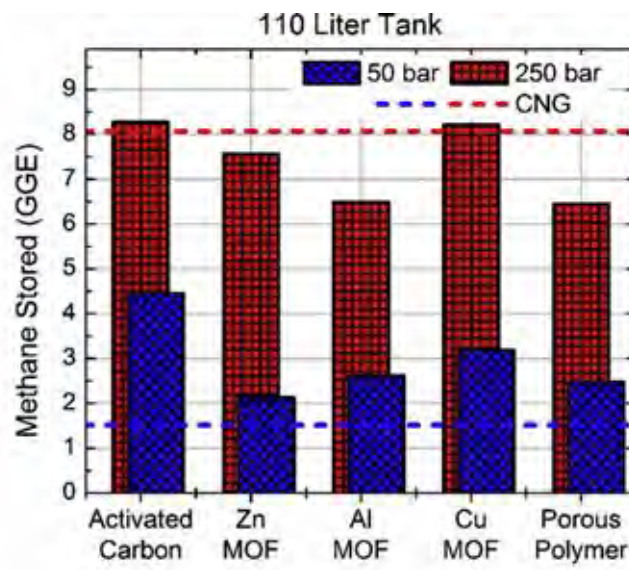


Figure 2.5 Methane stored of various activated carbon compare with compressed gas storage (Beckner *et al.*, 2015).

2.6.2 Effect of Oxygen-Containing Functional Groups on Several Type Adsorbent

Chiang *et al.*, (2002) studied the effect of ozone and alkaline treatment on activated carbon. The samples properties were elucidated in terms of surface functional groups and surface acidity. Surface functional groups were analyzed by fourier transform infrared spectroscopy (FTIR) and Boehm's titration. The surface acidity of activated carbon was determined by electrophoretic mobility measurements. The experiment date present that oxygen concentration of activated carbon increased after ozone and NaOH treatment. Surface functional groups increased mostly in the hydroxyl and carboxyl categories rather than the carbonyl category.

Chen and Wu (2004) applied the physicochemical methods to modify the surface of activated carbon by HCl, HNO₃ and NaOH. In addition, the effects of surface modification on the activated carbon properties, such as specific surface area (SSA), total acidity capacity, and carbon pH were investigated. The results of HCl, HNO₃, and NaOH treatment caused a significant change in the carbon chemical properties including the carbon pH and total acidity capacity. However, there was no

change in the SSA of the carbons. According to the XPS and FTIR results, they showed that with the HNO₃ treatment, the activated carbon produced a significantly increase of surface functional groups, which included carbonyl, carboxyl, and nitrate groups, whereas the NaOH treatment caused the increase in the hydroxyl group content. In addition, the HCl treatment caused the increase in the amount of single-bonded oxygen functional groups which included ethers, lactones, and phenols.

Xiao et al., (2008) treatment the activated carbon by HNO₃, H₂SO₄, and H₂ used for methane storage. The properties of the samples were studied by nitrogen adsorption, temperature-programmed desorption (TPD), Boehm titration, and Fourier transform infrared (FTIR) spectroscopy. The methane adsorption was measured by gravimetric difference apparatus. It was found that surface treatment significantly influenced the surface properties and pore structures of the activated carbon. The surface area and pore volume were enhanced by acid treatment resulted in the removal of impurities but for H₂ treatment surface area and porosity were reduced, oxygen containing functional groups on the surface would be consumed and lead to a weakened or even destroyed pore wall. Methane sorption capacity did increase slightly in acid treatment samples relate to the surface area. H₂ treatment not only decreased the surface area and porosity but also changed surface properties, which decreased methane storage capacity.

Derylo-Marczewska *et al.*, (2010) studied the effect of oxygen groups on adsorption of benzene derivatives from aqueous solution onto activated carbon. The commercial granular active carbon (Norit R3ex) was modified by two different processes (i) oxidation by Nitric acid (HNO₃) (ii) removal of external layers from granules by attrition. In terms of nitrogen adsorption/desorption isotherms found that the half width of micropores increases significantly after oxidation process, while the surface area and micropore volume decrease during attrition. The isotherms of nitrobenzene, phenol, 4-nitrophenol and 4-chlorophenol adsorption from dilute aqueous solutions on the non-modified and oxidized carbon samples are compared. In the case of nitrobenzene and phenol much stronger adsorption is observed on the non-modified carbon. Decreasing of adsorption on the oxidized sample results from two effects: (i) the presence of oxygen functional groups on carbon surface which show higher affinity towards water molecules and block the pore space (ii) from the electron-

withdrawing properties of carboxylic surface groups which weaken the dispersive interactions, both effects reduce adsorption of organic molecules from aqueous solution. Finally, they concluded that the adsorption effectiveness was regarded as a result of the differences in adsorbate hydrophobicity and the effect of specific interactions of its functional groups with active sites on carbon surface.

Lin Li *et al.*, (2011) studied chemically surface modification of coconut shell based activated carbon for improving hydrophobic volatile organic compounds (VOCs) adsorption. Granular activated carbon (GAC), prepared from coconut shell was using for starting material were chemical treated made with ammonia, sodium hydroxide, nitric acid, sulphuric acid and phosphoric acid. Adsorption capacity was tested with dry air stream mixing known concentrated O-Xylene. GAC with alkali-treated improve adsorption compared to original while the GAC modified by acid has less adsorption capacity. Also, Surface functional groups such as phenolic group ($-OH$), carbonyl group (CO), and carboxylic group ($-COOH$) were determined by Boehm titration. The results of these surface functional groups are shown in Figure 2.16.

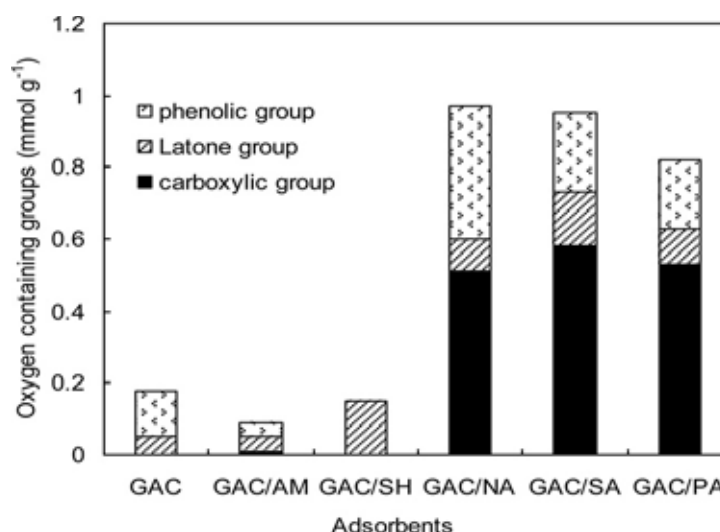


Figure 2.6 Surface functional groups of various activated carbon (mmol/g) (Li *et al.*, 2011).

The results present of oxygen containing functional group increased when strong oxidation with acid as the major of oxygen group is carboxylic on the other hand total concentration of oxygen group decreased by alkali-treating, occurred mostly on the

phenolic group. The adsorption capacity for o-xylene increased with the increase in surface area, total pore volume, and surface hydrophobicity. Modification by ammonia can improve the surface area and decreased the concentration of surface oxygen groups. The removing surface oxygen group as well as reducing hydrophilic carbon surface favors adsorption capacity of hydrophobic VOCs on carbon.

lu *et al.*, (2012) studied the surface modification of coconut activated carbon (ACs) by using chemical methods with different concentration of nitric acid oxidation at 25°C to produce oxygen functional group to enhance adsorption capacity of sodium and formaldehyde. The result from Scanning electron micrograph (SEM) showed the morphology of activated carbon after oxidation some pore widening. The samples which oxidation by the high concentration of nitric acid results in eroded and the pore blockage in the micropores be consistent with the decreased of surface area and pore volume. From Boehm method was appeared the increasing of concentration of nitric acid, the amount of carboxylic group and phenolic group was increased. Fourier transform infrared spectroscopy (FTIR) was used to investigate functional groups. The presence of more -OH groups, -COOH groups in the oxidized ACs. The capacity of adsorption of sodium in oxidized carbon higher than unmodified ACs because of the increasing of carboxylic and phenolic acid functionality in oxidized ACs, the adsorption capacity of formaldehyde increases from 11.5% to 24.2% after oxidation modified. It is indicated that chemical properties of activated carbon played an important role in adsorption capacity of activated carbon.

Feng *et al.*, (2013) studied the role of oxygen containing functional group on coal surface for methane adsorption. The bituminous coal was treated by H₂SO₄, (NH₄)₂S₂O₈, and the mixture of H₂SO₄/(NH₄)₂S₂O₈ to familiarize the O-containing functional groups. Boehm titration was used to measure the quantities of oxygen containing group. The results of analysis, Boehm titration and X-ray photoelectron spectroscopy (XPS) showed that there were increases in terms of both the content of oxygen and the quantities of O-containing groups over the modified coals surface, particularly for the carboxyl group. From nitrogen adsorption results, the modified coals can present higher surface area and pore volume than untreated coal. The methane adsorption isotherms were determined by volumetric apparatus under pressure 4.0 MPa at 298 K and the result fitted well by Langmuir model. The

adsorption capacity decreased after oxidation treatment because the increasing quantities of oxygen containing groups. They concluded that oxygen group made the coal surface more hydrophilic and decrease amount of adsorption sites available for methane molecules.

Hao *et al.*, (2013) researched on the influence of oxygen functional group on methane adsorption onto coal. The bituminous coal used for starting material which is modified by oxidation with H_2O_2 , $(\text{NH}_4)_2\text{S}_2\text{O}_8$ and HNO_3 at room temperature. The textural characteristics were studied by nitrogen adsorption on a regular surface area analyzer. The results showed after oxidation with H_2O_2 or $(\text{NH}_4)_2\text{S}_2\text{O}_8$ or 2 mol/L HNO_3 the activated carbon sample texture did not much change, although the surface area, total pore volume and micropore volume slightly decreased as a result of oxidation. It significantly different with 4 mol/L HNO_3 oxidation the surface area, total pore volume and micropore volume decreased by 72.3%, 69.8% and 67.1% respectively. As expected, nitric acid is a strong oxidizing agent and the higher its concentration is, the stronger its oxidation introduced more oxygen groups blocking pore. X-ray photoelectron spectra (XPS) data showed the oxygen functional group increase after oxidation with acid. The methane adsorption capacity measured by the volumetric method at 303 K in pressure range 0-5.3. The result suggests that adsorption capacity decrease in oxidized samples while compared with the unmodified sample as well as positive correlation between methane adsorption capacity and the micropore volume. They found that coal with a higher amount of oxygen group and consequently with less hydrophobic character had lower methane adsorption capacity.

Van *et al.*, (2013) investigated of surface modification for introducing carboxylic group onto the surface of carbon nanotubes (CNTs). Starting with Multi-walled carbon nanotube (MWCNTs) were treated by the mixture of acid $\text{H}_2\text{SO}_4/\text{HNO}_3$ to introduce the carboxylic group that was applied to be the precursor in functionalization to produce amine and silane functional groups. The properties of CNTs were characterized by Fourier transform infrared (FTIR) spectroscopy, Raman spectroscopy, differential scanning calorimetry and thermal gravimetric analysis (DSC/TGA) and transmission electron microscopy (TEM) methods. From the results, the content of COOH group on the surface of MWCNTs increases with increasing

reaction time from 3.18% for 2h to 9.39% for 6h. the content of dodecylamine (DDA) and 3-aminopropyl triethoxysilane (3-APTES) are 34.8% and 19.7%.

Vega *et al.*, (2013) investigated the effect of oxygen functional groups of activated carbon (AC) on the adsorption of volatile sulphur compounds; ethyl mercaptan(ETM), dimethyl sulphide (DMS) and dimethyl disulphide (DMDS). Steam activated extruded RB3 carbon from Norit was used as raw material obtain a particle size between 63 and 212 μm . Chemical modifications were done by nitric oxidation, ozone oxidation in gas phase and aqueous phase. The chemical temperature programme desorption and X-ray photoelectron spectroscopy were applied to characterize the properties of AC. The modifications with nitric acid and ozone oxidation produced textural properties changes of AC as well as improving the oxygen containing group onto AC treated with nitric acid presented higher oxygen functional groups than ozone oxidation. The incorporation of oxygen functional groups brings about to increase the adsorption capacity of AC by the incorporation of hydroxyl functional groups in the case of ETM and DMS due to the hydrogen bond interactions. On the contrary, the studied treatments did not produce any increase in the DMDS adsorption.

CHAPTER III

EXPERIMENTAL

3.1 Materials and Equipment

3.1.1 Adsorbent

Commercial activated carbon (20-40 mesh bituminous coal-based activated carbon supported by Right Solution Co., Ltd.)

3.1.2 Gases

- The ultra-high purity (UHP) methane (99.999% purity purchased from Labgaz Thailand Co., Ltd.) was used for methane adsorption experiment.
- The high purity helium (99.99% purity purchased from Labgaz Thailand Co., Ltd.) was used for volumetric apparatus.

3.1.3 Chemicals

- Sodium hydroxide (99 % purity purchased from RCI Labscan Ltd.)
- Potassium hydroxide (85 % purity purchased from RCI Labscan Ltd.)
- Hydrogen peroxide (35 % purity purchased from RCI Labscan Ltd.)
- Sulfuric acid (98 % purity purchased from RCI Labscan Ltd.)
- Ammonium solution (30 % purity purchased from RCI Labscan Ltd.)
- Sodium ethoxide (95 % purity purchased from T.S. Inter lab Ltd.)
- Sodium carbonate (from RCI Labscan Ltd.)
- Sodium bicarbonate (from RCI Labscan Ltd.)
- Phenolphthalein indicator (from RCI Labscan Ltd.)
- Methyl red indicator (from RCI Labscan Ltd.)

3.1.4 Equipment

- Volumetric apparatus
- Surface area analyzer (SAA), Quantachrom/ Sorptomatic 1990
- Fourier transform infrared spectrophotometer (FTIR)

3.2 Experimental Procedures

3.2.1 Activated Carbon Characterizations

3.2.1.1 *Brunauer-Emmett-Teller (BET) Surface Area Analysis*

Surface area, micropore volume, total pore volume, and average pore diameter of the samples were elucidated by using Quantachrome/ Sorptomatic 1990 surface analyzer. Prior to analysis, the samples were outgassed under vacuum at 300 °C for approximately 10 hr. Then, the adsorbent was analyzed by nitrogen adsorption isotherms at boiling liquid nitrogen temperature (-196 °C).

3.2.1.2 *Fourier Transform Infrared Spectroscopy (FTIR)*

Nicolet, Nexus 670 Fourier transform infrared spectroscopy (FTIR) was applied to qualitatively estimate the chemical structure of activated carbon samples. The activated carbon samples were mixed with KBr by agate mortar. Then, the mixture was compressed under high pressure for the preparation of KBr pellets. The IR spectrum was obtained measured over a frequency between 400 to 4000 cm^{-1} .

3.2.1.3 *Boehm Titration*

The activated carbon was dehydrated in the oven at 110 °C for overnight. After degassing, 1 g of activated carbon was soaked in 25 ml of each solution 0.1 M NaOC_2H_5 , 0.1 M NaOH, 0.05 M Na_2CO_3 and 0.1 M NaHCO_3 . The mixtures were shaken for 24 h and then the solid part was filtered out. The filtered solution was then titrated with 0.1 M HCl. Phenolphthalein and methyl red were used as the indicator (Boehm, 1966).

3.2.2 Adsorption Measurement

3.2.2.1 *Sample Preparation*

Activated carbon samples in this study were commercial activated carbon (20-40 mesh bituminous coal-based activated carbon) and activated carbon modified by chemical treatments. At first, activated carbons were degassing in the oven at 110 °C for 24 h. For each experiment, 1.0-1.5 g of degassed activated carbons were put into the sample holder instantly. The weight of sample holder was recorded before and after filled with activated carbon to find the genuine weight of activated carbon in sample holder. After all, the sample holder was put on the volumetric apparatus.

3.2.2.2 *Adsorption Experiments*

The volumetric apparatus was applied to determine methane adsorption capacity. The figure 3.1 was apparatus components diagram. In this experiment, sample holder was a high pressure stainless steel reactor contact with K-type thermocouple for measuring the temperature of gas. Ultra high purity methane (99.999% purity) and high purity helium (99.99% purity) was used in this experiment. The pressure of system was measured by pressure transducer in the range of 0 to 3,000 psig with 0.13% error.

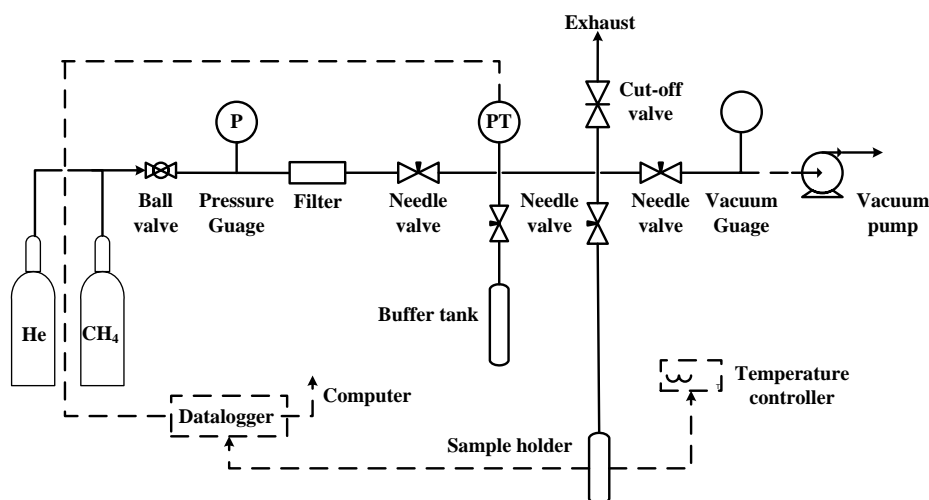


Figure 3.1 Schematic of the volumetric apparatus.

Rotary vacuum pump was applied to calibrate the pressure transducer and system degassing for each adsorption experiment. The vacuum pressure at -11.25 psi was used as the reference pressure. With this pressure, the comparative was set to zero under vacuum condition. The temperature was controlled to be constant at 35 °C throughout the experiment.

At first, the volume of the sample holder was determined by helium expansion based on the assumption that no helium was adsorbed on the adsorbents. The pressures and temperature were recorded before and after helium expansion.

Ideal Gas Law was used for calculate the volume of instrument total system (V_2 , volume of instrument after helium expansion).

$$\frac{P_1 V_1}{T_1} = \frac{P_2 V_2}{T_2} \quad (3.1)$$

- Where:
- P_1 = Pressure of helium before helium expansion
 - V_1 = Volume of the system excluding volume of sample holder
 - T_1 = Temperature before helium expansion
 - P_2 = Pressure of helium after helium expansion
 - V_2 = Total system volume, $V_1 + V_{\text{sample holder}}$
 - T_2 = Temperature after helium expansion

After measuring the volume of sample holder, the system was degassed by vacuum pump. During the experiment, the final pressure of methane in the sample holder was increased from less than 100 up to 1,000 psia. At desired pressure, methane was fed from a high-pressure cylinder into the system, the pressure was recorded before open the valve to sample holder. Afterwards methane expanded into a sample holder, the time to reach methane adsorption equilibrium was within approximately 30 min. Then final pressure of methane was recorded.

The ideal gas law and conservation of mass law were also applied for calculate the amount of methane adsorbed on the adsorbents by the following equation.

$$n_{ad} = n_{ad-1} + \left[\frac{P_i V_1}{zRT_i} - \frac{P_{f-1} V_2}{zRT_{f-1}} - \frac{P_f (V_1 + V_2)}{zRT_f} \right] \quad (3.2)$$

- Where:
- n_{ad} = Total amount of methane adsorbed by activated carbons (mole)
 - n_{ad-1} = Amount of methane adsorbed at previous stage (mole)
 - P_i = Initial pressure of methane before methane expansion (psia)
 - P_{f-1} = Final pressure of methane after methane expansion in the previous stage (psia)
 - P_f = Final pressure of methane after methane expansion (psia)
 - V_1 = Volume of system excluding volume of sample holder (cm^3)
 - V_2 = Volume of the sample holder (cm^3)
 - Z = Compressibility factor of methane
 - T_i = Initial temperature of methane before methane expansion (K)
 - T_f = Final temperature of methane after methane expansion (K)
 - T_{f-1} = Final temperature of methane after methane expansion into the sample holder in the previous stage (K)
 - R = Gas constant, $82.0578 \text{ atm}\cdot\text{cm}^3/\text{mol}\cdot\text{K}$

3.2.3 Activated Carbon Surface Treatment

3.2.3.1 *Ash Removal*

60 g of activated carbon was soaked in 250 ml of acids mixture solution composed by HCl, HF and H₂O at the ratio of 45:15:40 for 5 h at 70 °C. Then, the activated carbon was filtered and washed with distilled water until a pH was stable. The wet activated carbon was dried in oven at 110 °C for 24 h.

3.2.3.2 *Modifications of Activated Carbons*

The acidic and alkaline solution 10M NaOH, 10 M KOH, 9 M H₂SO₄, and 30% NH₃·H₂O 100 ml was added to 10 g of the deashed activated carbon at 70°C 2 h and then keep stirring at 35°C for 24 h. The 30% H₂O₂ 100 ml was added to 10 g of deashed activated carbon at room temperature and kept for 24 h. The modified activated carbon was separated by filtered and washed continually with distilled water. Finally, they were dried in oven at 110 °C for 24 h.

CHAPTER IV

RESULTS AND DISCUSSION

4.1 Activated Carbon Characterizations

4.1.1 Surface Area Analysis of Activated Carbons

In this study, commercial activated carbons and modified activated carbon were characterized prior to the methane adsorption study. The specific surface area (BET surface area), the micropore volume (Dubinin-Radushkevich, DR method), total pore volume, and average micropore diameter (Horvath and Kawazoe method) were conducted by using a Quantachrome/ Sorptomatic 1990 surface analyzer at liquid nitrogen temperature (-196 °C) as mentioned in 3.2.1.

Table 4.1 BET surface area, micropore volume, total pore volume and average micropore diameter of studied activated carbons

Adsorbents	Physical Characterization			
	BET Surface area (m ² /g)	Micropore volume (cm ³ /g)	Total pore volume (cm ³ /g)	Average micropore diameter (Å)
AC/Untreated	999.6	0.51	0.72	8.56
AC/De-ash	1007.6	0.48	0.76	7.85
AC/NaOH	976.8	0.46	0.67	7.77
AC/KOH	996.3	0.50	0.75	8.82
AC/NH ₃ ·H ₂ O	912.2	0.47	0.75	8.82
AC/H ₂ SO ₄	1048.7	0.53	0.65	8.10
AC/H ₂ O ₂	965.6	0.46	0.66	7.53

Table 4.1 summarized the BET surface area, micropore volume, total pore volume and average pore diameter of the activated carbon samples. The BET surface area of deashed activated carbon (AC/De-ash) is relatively constant as the

original activated carbon (AC/Untreated) (999.6 m²/g and 1,007.6 m²/g) and total pore volume slightly increased from 0.72 to 0.76 cm³/g possibly because the mix acids solution removes the impurities on the surface which blocks the pores of activated carbons. The surface area from the AC modified by alkalis are 986.9 m²/g for AC/NaOH and 912.2 m²/g for AC/NH₃.H₂O, which are lower than BET surface areas of AC/Untreated. For the AC/H₂O₂, the surface area and micropore volume are decreased, suggesting that micropore structure may be destroyed after the treatment. However, the strong acid treated activated carbon (AC/H₂SO₄) has the highest surface areas 1048.7 m²/g.

4.1.2 Infrared Spectroscopy Characterization of Activated Carbons

Fourier transform infrared spectroscopy (FTIR) was applied to qualitatively compare the function groups on the surface of activated carbon between before and after treatments. The IR spectra were collected using a Nicolet, Nexus 670 FTIR spectrometer. The activated carbon samples were prepared in form of KBr pellets. The IR spectrum was obtained over a frequency between 400 and 4,000 cm⁻¹. The FTIR spectra of AC/Untreated, AC/Deash, AC/NaOH, AC/KOH, AC/NH₃.H₂O, AC/H₂SO₄ and AC/H₂O₂ are presented in Figure 4.1. All samples exhibit broad band between 3,600-2,500 cm⁻¹, which is due to O-H stretching for phenolic and carboxylic group. The band at 1,700 cm⁻¹ should be ascribed to the stretching of C=O for carboxylic and lactone group. The band appear around 1,000-1,370 cm⁻¹ are associated with C-OH stretching, C-O-C stretching and O-H bending. However, the band at 3,435 cm⁻¹ for OH stretching is lower after treated by NaOH and NH₃.H₂O, and this observation is further confirmed by Boehm titration in the next section.

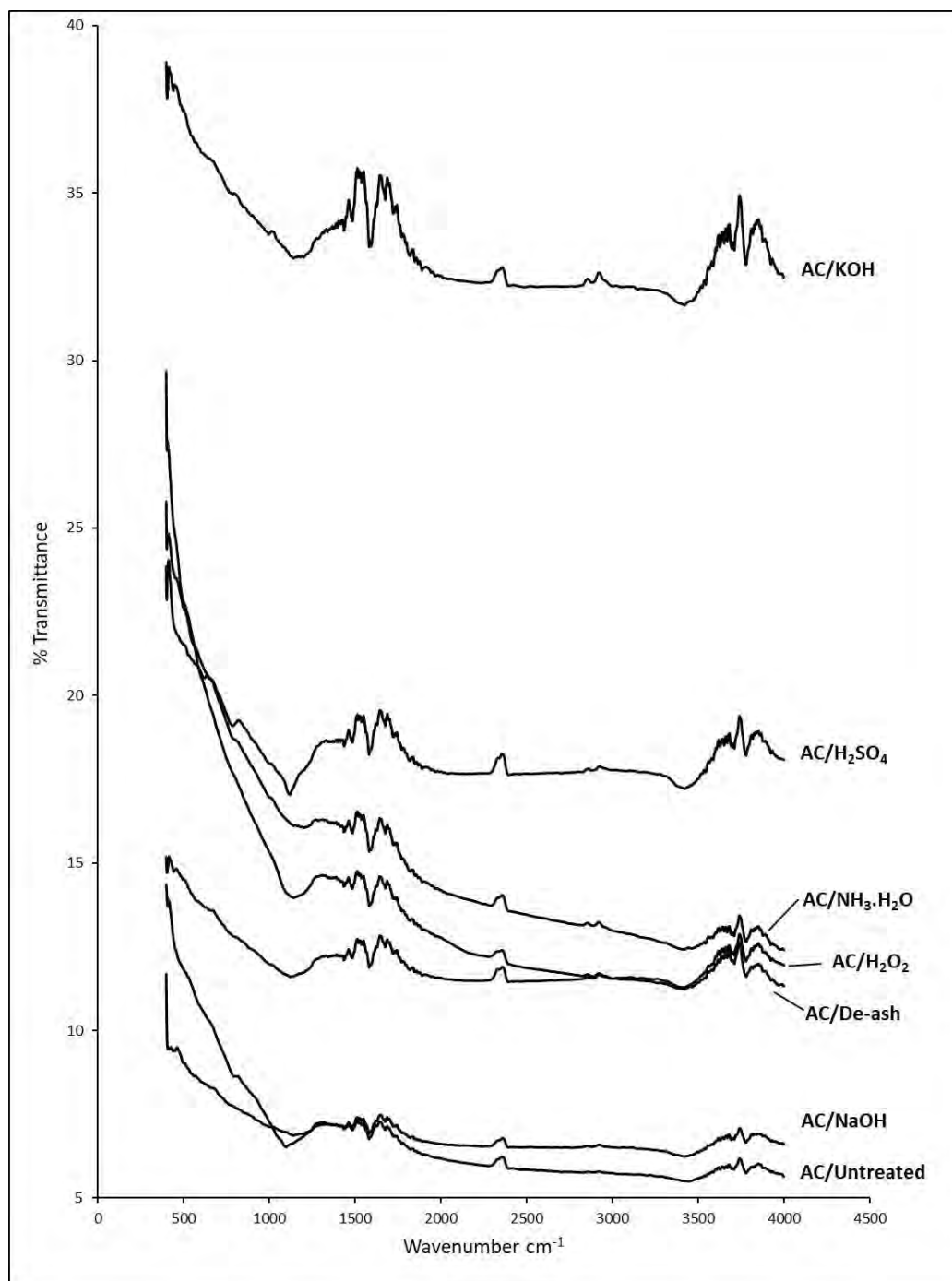


Figure 4.1 FTIR spectra of the treated and untreated activated carbons.

4.1.3 Boehm Titration

The oxygen-containing functional group such as phenolic, ketone and carboxylic groups on activated carbons surfaces can be quantified by Boehm titration

method as mentioned in section 3.2.3. The oxygen-containing functional groups is possibly derived from the chemical treatment and the quantities of each group are summarized in Table 4.3 and Figure 4.1. For AC/De-ash, the total oxygen containing functional group is 0.379 mmol/g with 87.6% (0.332 mmol/g) of phenolic group, 8.4% (0.032 mmol/g) of lactone groups and 3.9% (0.015 mmol/g) of carboxylic group. After treated AC/De-ash with strong bases, the total concentration of oxygen containing functional groups is decreased slightly from 0.379g mmol/g to 0.350 mmol/g for AC/NaOH and 0.365 mmol/g for AC/KOH, and carboxylic group is disappeared. Similarly, the treatment with $\text{NH}_3 \cdot \text{H}_2\text{O}$ causes the total amount of these oxygen-containing functional groups decreasing to 0.345 g mmol/g. On the other hand, the total concentration of oxygen containing functional groups increased dramatically when the activated carbon was modified by H_2SO_4 and H_2O_2 (from 0.379 mmol/g to 0.654 mmol/g and 0.734 mmol/g) and this increasing is mostly due to the phenolic group.

Table 4.2 Quantification of oxygen-containing functional groups by Boehm titration

Adsorbent	Amount of oxygen-containing functional groups (mmol/g)			
	Carboxylic	Lactone	Phenolic	Total
AC/De-ash	0.015	0.032	0.332	0.379
AC/NaOH	0	0.005	0.345	0.350
AC/KOH	0	0.060	0.305	0.365
AC/ $\text{NH}_3 \cdot \text{H}_2\text{O}$	0.015	0.015	0.315	0.345
AC/ H_2SO_4	0.140	0.045	0.470	0.654
AC/ H_2O_2	0.120	0.035	0.580	0.734

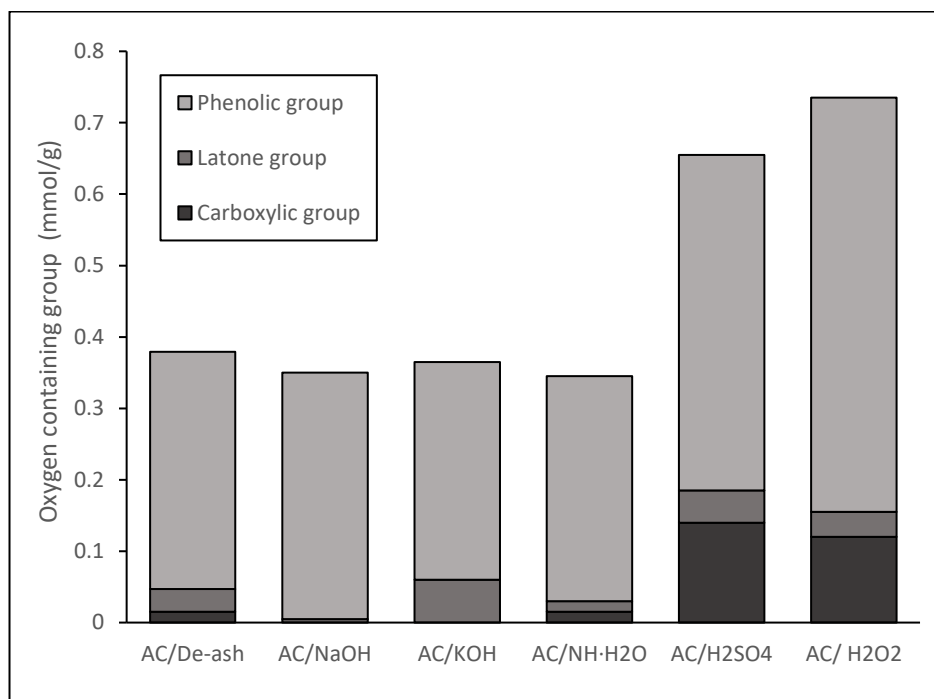


Figure 4.2 Specific amount of oxygen-containing functional groups on surface of activated carbon samples.

After acids treatment, more oxygen-containing functional groups are emerged. The contents of all samples are mainly the phenolic group which is between 79.0 % to 98.6 % of total oxygen functional contain. AC/H₂O₂ shows highest amount of total oxygen on the surface possibly due to the fact that H₂O₂ is a very strong oxidizing agent.

4.2 Adsorption of Methane on Modified and Un-modified Activated Carbon

The methane adsorption capacities of activated carbon samples were elucidated by the volumetric apparatus with the pressure up to 1,000 psia of ultra-high purity methane (99.999% purity) at 35°C. Figure 4.2 shows the methane adsorption capacity of the prepared activated carbon. The methane adsorption isotherm was plotted between the amount of methane (mmol) per gram of activated carbon and equilibrium pressure of methane (psia). As expected, the methane adsorption increases with increasing methane's pressure. The methane adsorption capacity of ash removal

and surface treated activated carbon was greater than the original commercial activated carbon. The NaOH modification activated carbon; AC/NaOH present the highest amount of methane adsorption, following by AC/De-ash, AC/NH₃·H₂O, AC/H₂SO₄, AC/H₂O₂, AC/KOH, AC/Untreated.

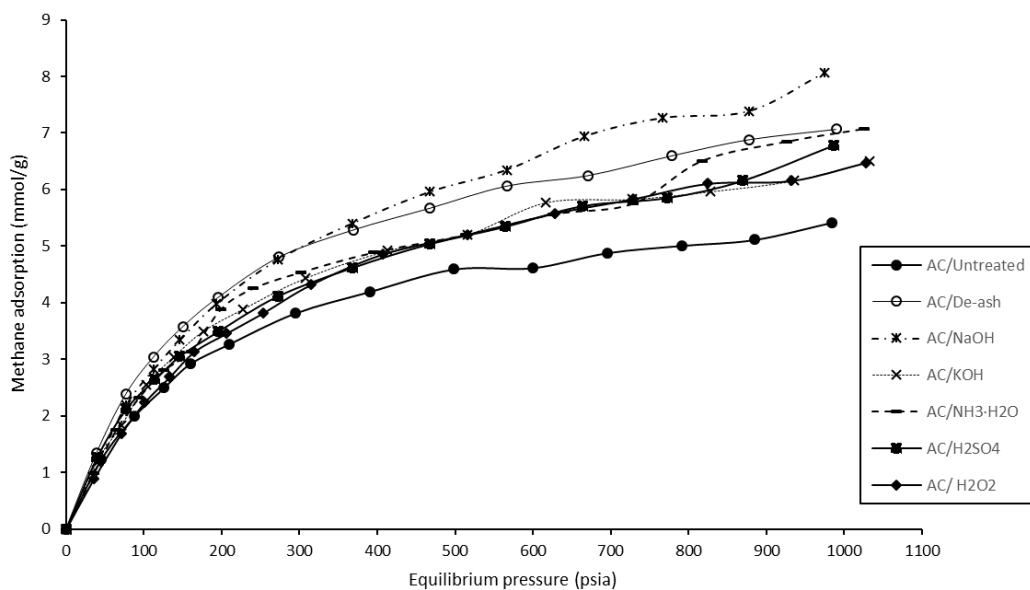
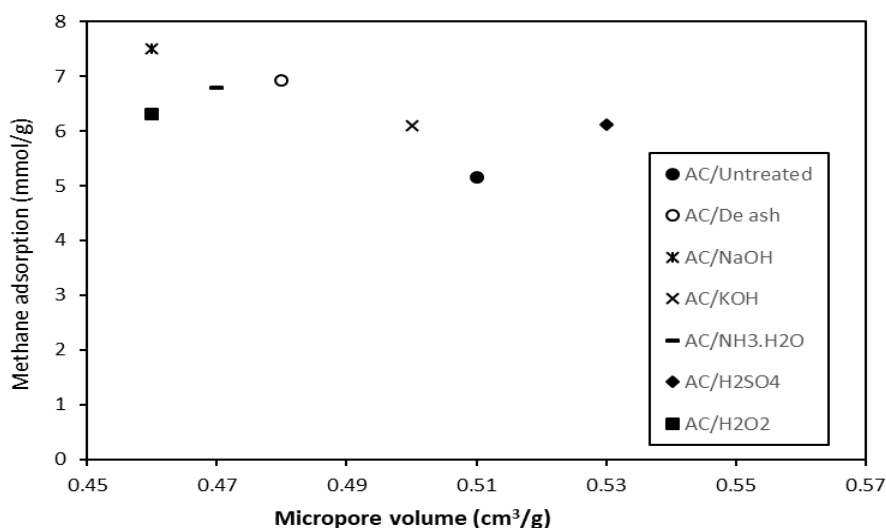


Figure 4.3 Methane adsorption capacity (mmol/g) on activated carbon samples at 35 °C.

Table 4.3 Methane adsorption capacity (mmol/g) of adsorbents at 900 psia and 35 °C

Adsorbent	Methane Adsorption (mmol/g) at 900 psia and 35 °C
AC/Untreated	5.15
AC/De-ash	6.92
AC/NaOH	7.50
AC/KOH	6.09
AC/NH ₃ ·H ₂ O	6.79
AC/H ₂ SO ₄	6.11
AC/H ₂ O ₂	6.30

Figures 4.4-4.7 show relation between the methane adsorption capacity at 900 psia, 35 °C and micropore volume, total pore volume, DR pore diameter and, BET surface area respectively. Remarkably, in this study micropore volume, total pore volume, and DR pore diameter and BET surface area have no effect on methane absorption for activated carbon.

**Figure 4.4** Methane adsorption capacity (mmol/g) at 900 psia and 35 °C as a function of micropore volume (cm³/g).

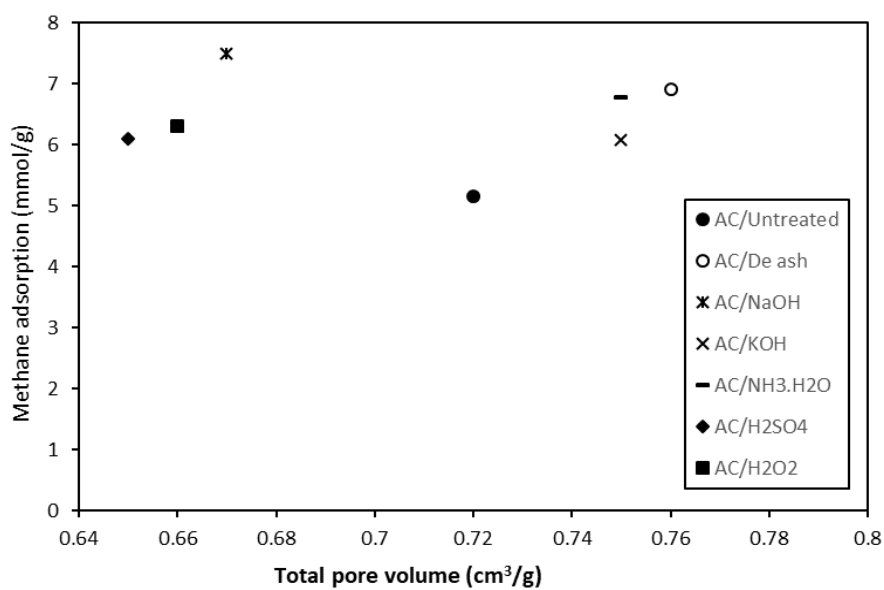


Figure 4.5 Methane adsorption capacity (mmol/g) at 900 psia and 35 °C as a function of total pore volume (cm³/g).

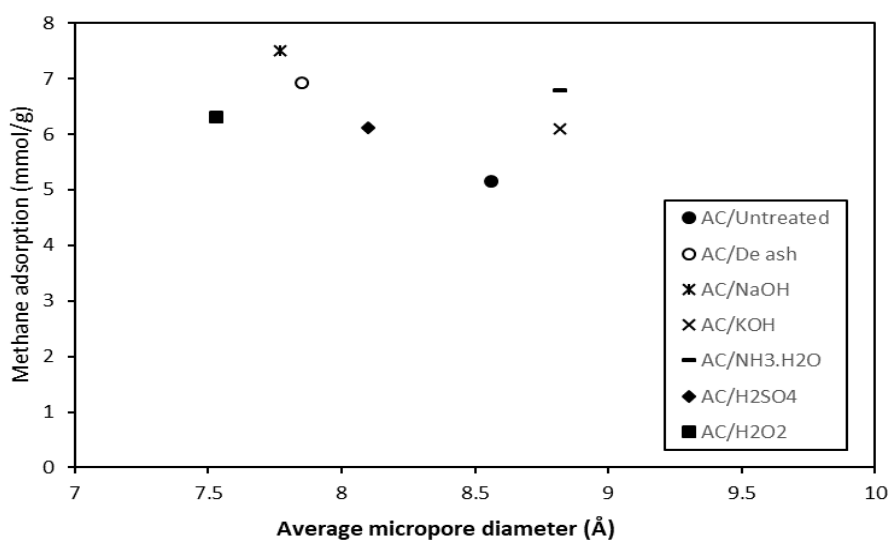


Figure 4.6 Methane adsorption capacity (mmol/g) at 900 psia and 35 °C as a function of Average micropore diameter (Å).

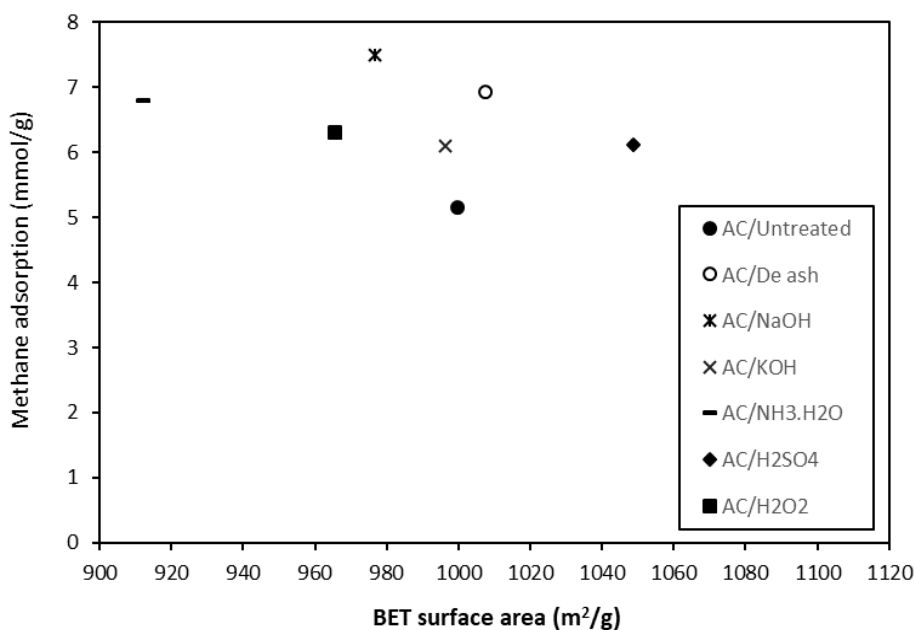


Figure 4.7 Methane adsorption capacity (mmole/g) at 900 psia and 35 °C as a function of BET surface area (m²/g).

According to previous studies, (Sunthonsuriyawong, 2013) and (Seangnak, 2014) the BET surface area and the amount of methane adsorption could be described as linear relationships. Higher surface area generally provides higher adsorption capacity.

However, the chemical property on the surface of activated carbon could play an important role in the adsorption of methane. Li et al, 2011 also explained the overall performance of adsorbent depends on several factors; surface area, pore size and carbon surface chemistry.

Figure 4.8 the methane adsorption isotherm shows the relationship between methane adsorption capacity per adsorbent surface area (m²) and equilibrium pressure. The results show the difference of methane adsorption per unit area which could explain that not only surface area plays the important role to methane adsorption but also other factors.

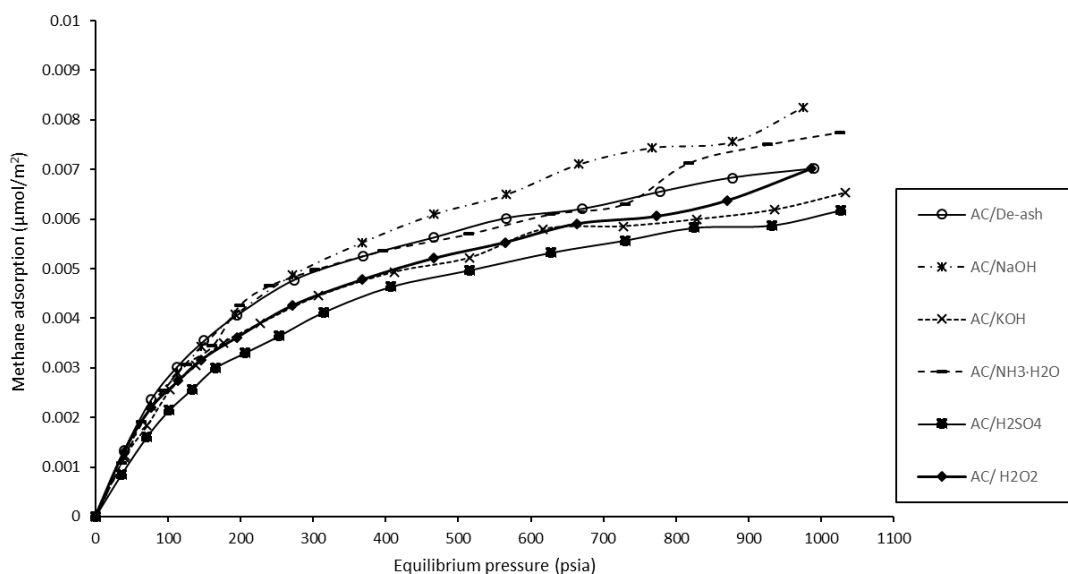


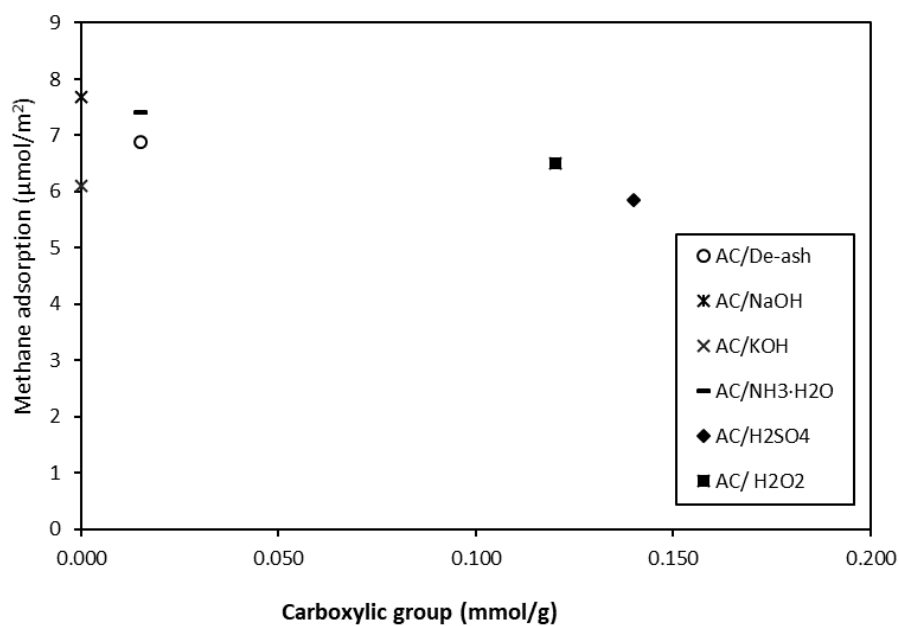
Figure 4.8 Methane adsorption capacity ($\mu\text{mol}/\text{m}^2$) on activated carbons samples at $35\text{ }^\circ\text{C}$.

From the methane adsorption capacity at the same unit of BET surface area ($\mu\text{mol}/\text{m}^2$), the activated carbon treated by NaOH and $\text{NH}_3\cdot\text{H}_2\text{O}$ which had less BET surface area presented the high methane adsorption capacity. The AC/NaOH was the highest of both methane adsorption either per BET surface area and per gram. The NaOH modification could be suitable for methane adsorption due to the highest adsorption capacity.

However, AC/ H_2SO_4 which has highest BET surface presents the lowest capacity of methane adsorption per 1 m^2 of BET surface area.

Table 4.4 Methane adsorption capacity ($\mu\text{mol}/\text{m}^2$) of adsorbent at 900 psia and 35 °C

Adsorbent	Methane Adsorption ($\mu\text{mol}/\text{m}^2$) at 900 psia and 35°C
AC/De-ash	6.89
AC/NaOH	7.68
AC/KOH	6.1
AC/ $\text{NH}_3 \cdot \text{H}_2\text{O}$	7.41
AC/ H_2SO_4	5.86
AC/ H_2O_2	6.51

**Figure 4.9** Methane adsorption capacity ($\mu\text{mol}/\text{m}^2$) at 900 psia and 35 °C as a function of carboxylic group (mmol/g).

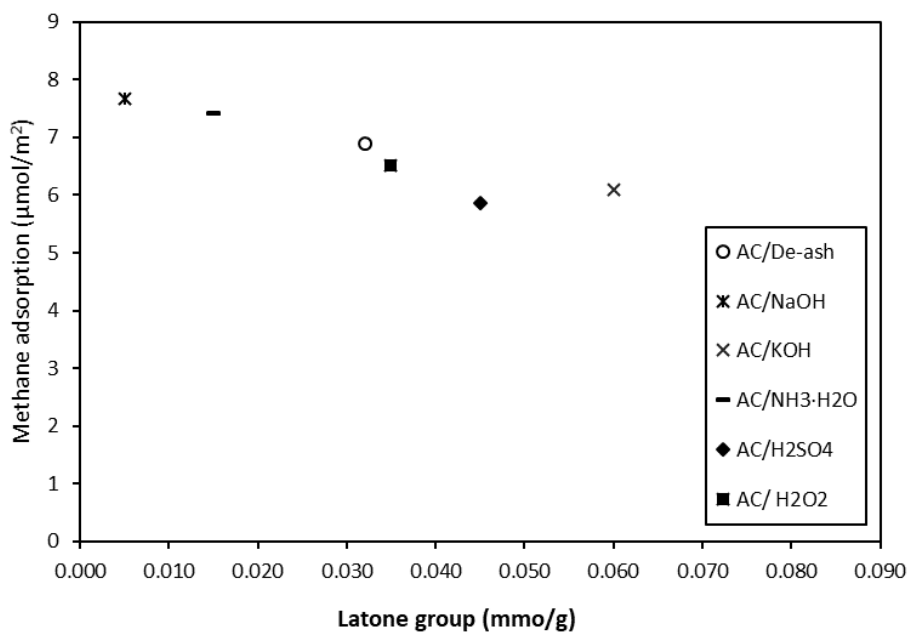


Figure 4.10 Methane adsorption capacity ($\mu\text{mol}/\text{m}^2$) at 900 psia and 35 °C as a function of latone group (mmol/g).

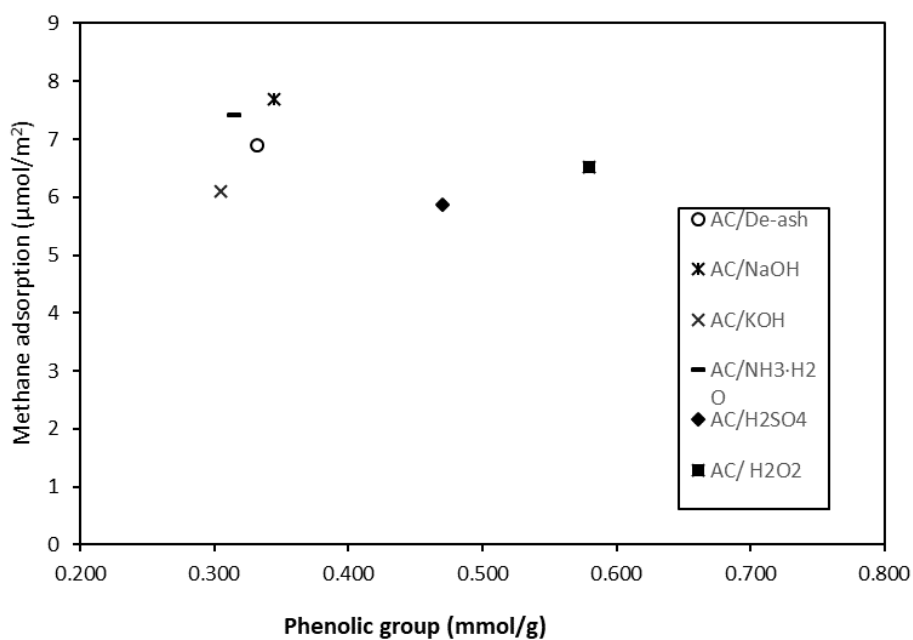


Figure 4.11 Methane adsorption capacity ($\mu\text{mole}/\text{m}^2$) at 900 psia and 35 °C as a function of phenolic group (mmol/g).

Figure 4.9 shows the relationship between methane adsorption capacity ($\mu\text{mol}/\text{m}^2$) at 900 psia and 35 °C and amount of carboxylic group on activated carbon surface. From the result, the carboxylic group on activated carbon surface was disappeared when treated with NaOH and KOH solutions. AC/De-ash and AC/ $\text{NH}_3 \cdot \text{H}_2\text{O}$ still presented small amount of carboxylic group at 0.015 mmol/g. Meanwhile, activated carbon treated by acid solutions presented high carboxylic group on the surface, AC/ H_2SO_4 had highest carboxylic group, also provides the lowest methane adsorption capacity.

Figure 4.10 shows the relationship between methane adsorption capacity ($\mu\text{mol}/\text{m}^2$) at 900 psia and 35 °C and amount of latone group on activated carbon surface. Activated carbon treated by NaOH contained lowest latone group and presented highest methane adsorption capacity. Although, AC/KOH contained less carboxylic group and phenolic group but also highest amount of latone group.

Figure 4.11 shows the relationship between methane adsorption capacity ($\mu\text{mol}/\text{m}^2$) at 900 psia and 35 °C and amount of phenolic group on activated carbon surface. The deashed activated carbon and alkali treated activated carbon present low amount of phenolic group, the activated carbon treated with KOH had lowest phenolic group. Meanwhile, the acid treatments activated carbon contained high phenolic group, especially the activated carbon treated by H_2O_2 .

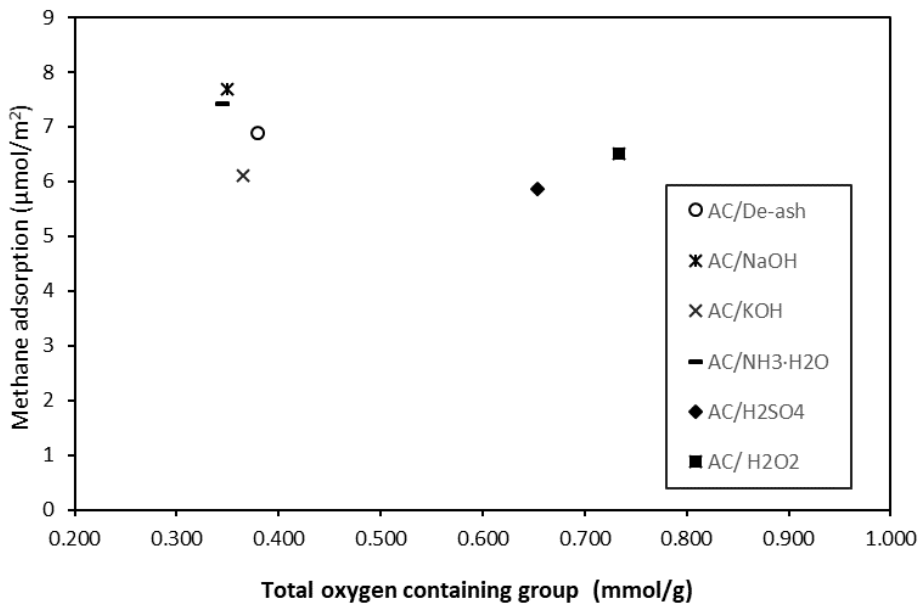


Figure 4.12 Methane adsorption capacity ($\mu\text{mol}/\text{m}^2$) at 900 psia and 35 °C as a function of total oxygen containing group (mmol/g).

Figure 4.12 shows the relationship between total oxygen-containing functional groups on activated carbon surface and methane adsorption capacity. The methane adsorption capacity of activated carbon treated with NaOH and $\text{NH}_3 \cdot \text{H}_2\text{O}$ is higher than deashed activated carbon due to its lower oxygen-containing functional groups, which was considered the reason for acidic property on the activated carbon surface. Moreover, high oxygen-containing functional groups were found in acid modification activated carbon, that presented low methane adsorption capacity. Therefore, the oxygen-containing functional groups on the surface of activated carbon might play an important role on the methane adsorption by activated carbon. On the other hand, the activated carbon treated by KOH presented low oxygen-containing functional groups but low methane adsorption capacity. Therefore, there would be another determinant which could have effect to methane adsorption as how Boehm, 1996 explained that the carbon surface containing several elements e.g., sulfur, chlorine and hydrogen that can affect to methane adsorption on activated carbon surface.

CHAPTER V

CONCLUSIONS AND RECOMMENDATION

5.1 Conclusions

The bituminous coal-based activated carbon modified by acid solution H_2O_2 and H_2SO_4 , which is oxidation treatment, engendered more oxygen-containing functional groups on the activated carbon surface and presented low methane adsorption capacity ($\mu\text{mol}/\text{m}^2$). Although, the alkali solution treatment by $NaOH$ and NH_3H_2O improved the methane adsorption capacity ($\mu\text{mol}/\text{m}^2$) were decreased the oxygen-containing functional groups on the activated carbon surface. Boehm titration and FTIR spectra results confirmed the presence of oxygen-containing functional groups on the activated carbon surface consisting of phenolic group, lactone group and carboxylic group occurred mostly on the phenolic group.

The highest methane adsorption at 900 psia 35 °C was 7.50 mmol/g and 7.68 $\mu\text{mol}/\text{m}^2$ by chemical surface modification with $NaOH$. From Boehm titration result, AC/ $NaOH$ showed the lowest amount of total oxygen-containing functional groups 0.350 mmol/g. AC/ H_2SO_4 had the lowest methane adsorption capacity per 1 m^2 of BET surface at 5.86 $\mu\text{mol}/\text{m}^2$ and exhibited high total oxygen-containing functional groups (0.654 mmol/g). Therefore, the oxygen-containing functional groups on the surface of activated carbon might play an important role on the methane adsorption. On the other hand, AC/ KOH presents the low oxygen-containing functional groups but lowest methane adsorption capacity per gram (6.09 mmol/g) implied that the amount of methane adsorption did not only depend on oxygen-containing functional groups but also other surface properties of carbon.

5.2 Recommendation

There is not only oxygen functional group present on activated carbon surface but also nitrogen groups, basic groups and end group which could present the different effect to methane absorption and still require more study to clarify.

REFERENCES

- Bagheri, N., and Abedi, J. (2011) Adsorption of methane on corn cobs based activated carbon. Chemical Engineering Research and Design, 89(10), 2038-2043.
- Baker, F.S., Miller, C.E., Repic, A.J., and Tolles E.D. (1992) Activated carbon. Kirk-Othmer Encyclopedia of Chemical Technology, 4, 1015-1037.
- Balathanigaimani, M.S., Kang, H-C., Shim, W-G., Kim, C., Lee, J-W., and Moon, H. (2006) reparation of powdered activated carbon from rice husk and its methane adsorption properties. Korean Chemical Engineering, 23(4), 663-668.
- Bastos-Neto, M., Canabrava, D.V., Torres, A.E.B., Rodriguez-Castellón, E., Jiménez-López, A., Azevedo, D.C.S., and Cavalcante, C.L. (2007) Effects of textural and surface characteristics of microporous activated carbons on the methane adsorption capacity at high pressures. Applied Surface Science, 253, 5721–5725.
- Beckner, M., and Dailly, A. (2015) Adsorbed methane storage for vehicular applications. Applied Energy, 149, 69-74.
- Boehm, H.P. (1996) Chemical identification of surface group. Advances in catalysis, 16, 179-274.
- Boehm, P., and Saba, T. (2009) Identification of natural gas sources using geochemical forensic tools. Environmental forensics notes, 5.
- Chen, JP., and Wu, S. (2004) Acid/Base-treated activated carbons: characterization of functional groups and metal adsorptive properties. Langmuir, 20(6), 2233.
- Chiang, H-L., Huang, C.P., and Chiang, P.C. (2002) The surface characteristics of activated carbon as affected by ozone and alkaline treatment. Chemosphere, 47, 257–265.
- Derylo-Marczewskaa, A., Buczekb, B., and Swiatkowskic, A. (2011) Effect of oxygen surface groups on adsorption of benzene derivatives from aqueous solutions onto active carbon samples. Applied Surface Science, 257, 9466-9472.
- El-Hendawy, A.A. (2003). Influence of HNO₃ oxidation on the structured and adsorptive properties of corncobs activated carbon. Carbon, 41, 713-722.

- Eftekhari, H., and Farzaneh-Gord, M. (2009) Producing compressed natural gas for natural gas vehicles by alternative and traditional ways. Iran: National Iranian Gas Company.
- Feng, Y., Yang, W., Liu, D., and Chu, W. (2013) Surface Modification of Bituminous Coal and Its Effects on Methane Adsorption. Chinese Journal of Chemistry, 31(8), 1102-1108.
- Hao, S., Wen, J., Yu, X., and Chu, W. (2013) Effect of the surface oxygen groups on methane adsorption on coals. Applied Surface Science, 264, 433-442.
- Jeong, B.M., Ahn, E.S., Yun, J.H., Lee, C.H., and Choi, D.K. (2007) Ternary adsorption equilibrium of H₂/CH₄/C₂H₄ onto activated carbon. Separation and Purification Technology, 55(3), 335-342.
- Li, L., Liu, S., and Liu, J. (2011) Surface modification of coconut shell based activated carbon for the improvement of hydrophobic VOC removal. Journal of Hazardous Materials, 192, 683-690.
- Lozano-Castelló, D., Alcañiz-Monge, J., De La Casa-Lillo, M.A., Cazorla-Amorós, D., and Linares-Solano, A. (2002) Advances in the study of methane storage in porous carbonaceous materials. Fuels, 81, 1777-1803.
- Lu, X., Jiang, J., Sun, K., Xie, X., and Hu, Y. (2012). Surface modification, characterization and adsorptive properties of a coconut activated carbon. Applied Surface Science, 258, 8247-8252.
- Lozano-Castelló, D., Cazorla-Amorós, D., Linares-Solano, A., and Quinn, D.F. (2002) Influence of pore size distribution on methane storage at relatively low pressure: preparation of activated carbon with optimum pore size. Carbon, 40, 989-1002.
- Lozano-Castelló, D., Lillo-Ródenas, M.A., Cazorla-Amorós, D., and Linares-Solano, A. (2001) Preparation of activated carbons from Spanish anthracite: I. activation by KOH. Carbon, 39, 741-749.
- Mochida, I., Koraiya, Y., Shirahama, M., Kawano, S., Hada, T., Seo, Y., Yoshikawa, M., and Yasutake, A. (2000) Removal of SO and NO over activated carbon fibers. Carbon, 38, 227-239.

- Najibi, H., Chapoy, A., and Bahman, T. (2008) Methane/natural gas storage and delivered capacity for activated carbons in dry and wet conditions. Fuel, 87, 7-13.
- Namvar-Asl, M., Soltanieh, M., Rashidi, A., and Irandoukht, A. (2008) Modeling and preparation of activated carbon for methane storage I. Modeling of activated carbon characteristics with neural networks and response surface method. Energy Conversion and Management, 49, 2471-2477.
- Rodríguez-Reinoso, F., Nakagawa, Y., Silvestre-Albero, J., Juarez-Galan, J.M., and Molina-Sabio, M. (2008) Correlation of methane uptake with microporosity and surface area of chemically activated carbons. Microporous and Mesoporous Materials, 115(3), 603-608.
- Rouquerol, F., Rouquerol, J., and Sing, K. (1999) Adsorption by Powder & Porous Solid. London: Academic Press.
- Seangnak, P. (2013) Comparative study for the effect of ozone treatment on activated carbon for methane adsorption, M.S. Thesis, The Petroleum and Petrochemical College, Chulalongkorn University, Bangkok, Thailand.
- Solar, C., Blanco, A.G., Vallone, A., and Sapag, K. (2010) Natural gas. Journal of Natural Gas Chemistry, pp 205–244, InTech.
- Soo-Jin, P., and Min-Kang, S. (2011) Solid-Gas Interaction. Interface Science and Composites, 70-104.
- Sunthonsuriyawong, W. (2013) Comparative study for Methane adsorption by activated carbons: comparison among coconut-, palm-, and bituminous coal based activated carbons, M.S. Thesis, The Petroleum and Petrochemical College, Chulalongkorn University, Bangkok, Thailand.
- Van, T.L., Cao, L.N., Quoc, T.L., Trinh, T.N., Duc, N.N., and Minh, T.V. (2013) Surface modification and functionalization of carbon nanotube with some organic compounds. Advances in Natural Sciences: Nanoscience and Nanotechnology, 4(3), 1-5.
- Vega, E., Lemus, J., Anfruns, A., Gonzalez-Olmos, R., Palomar, J., and Maria, J.M. (2013). Adsorption of volatile sulphur compounds onto modified activated carbons: Effect of oxygen functional groups. Journal of Hazardous Materials, 258-259, 77-83.

- Xiao, D.D., Xin, M.L., Zhao, G.F., Ling, Q., Ke, Q., and Zi, F.Y. (2008) Treatment of activated carbon for methane storage. Asia-Pacific Journal of Chemical Engineering, 3, 292-297.
- Zeng, X. and Osseo-Asare, K. (2001) Partition of pyrite and hematite in aqueous biphasic system: effects of pH and surfactants. Colloids and Surfaces A, 17, 247-254.
- Victorovich, B.A. "Adsorbed natural gas system for storage of natural gas and use in transport." CarbonCenter. 15 May 2016 <<http://carboncenter.ru/carbon-center/>>

APPENDICES

Appendix A Methane Adsorption on Each Studied Activated Carbon at 35 °C

Table A1 The amount of methane adsorption (mmol/g) on AC/Untreated

Equilibrium pressure (psia)	Methane adsorption (mmol/g)
0.00	0
45.00	1.230
88.13	1.997
125.63	2.494
159.38	2.919
210.00	3.271
294.38	3.814
390.00	4.193
498.75	4.592
600.01	4.616
695.63	4.880
791.25	5.008
885	5.112
984.38	5.417

Table A2 The amount of methane adsorption ($\mu\text{mol}/\text{m}^2$) on AC/Untreated

Equilibrium pressure (psia)	Methane adsorption ($\mu\text{mol}/\text{m}^2$)
0.00	0.000
45.00	1.231
88.13	1.998
125.63	2.495
159.38	2.920
210.00	3.272
294.38	3.815
390.00	4.195
498.75	4.593
600.01	4.617
695.63	4.882
791.25	5.010
885.00	5.114
984.38	5.419

Table A3 The amount of methane adsorption (mmol/g) on AC/De-ash

Equilibrium pressure (psia)	Methane adsorption (mmol/g)
0.00	0.000
39.38	1.346
76.84	2.381
112.50	3.041
150.00	3.575
195.00	4.088
273.75	4.807
369.38	5.288
466.88	5.669
566.25	6.062
671.25	6.250
778.13	6.597
877.50	6.883
990.00	7.068

Table A4 The amount of methane adsorption ($\mu\text{mol}/\text{m}^2$) on AC/De-ash

Equilibrium pressure (psia)	Methane adsorption ($\mu\text{mol}/\text{m}^2$)
0.00	0.000
39.38	1.336
76.84	2.363
112.50	3.018
150.00	3.548
195.00	4.058
273.75	4.770
369.38	5.248
466.88	5.626
566.25	6.017
671.25	6.203
778.13	6.547
877.50	6.831
990.00	7.015

Table A5 The amount of methane adsorption (mmol/g) on AC/NaOH

Equilibrium pressure (psia)	Methane adsorption (mmol/g)
0.00	0.000
41.25	1.203
76.88	2.191
112.50	2.830
146.25	3.342
193.13	3.980
271.88	4.761
367.50	5.401
466.88	5.959
566.25	6.347
665.63	6.941
766.88	7.266
877.50	7.383
975.00	8.063

Table A6 The amount of methane adsorption ($\mu\text{mol}/\text{m}^2$) on AC/NaOH

Equilibrium pressure (psia)	Methane adsorption ($\mu\text{mol}/\text{m}^2$)
0.00	0.000
41.25	1.231
76.88	2.243
112.50	2.897
146.25	3.422
193.13	4.075
271.88	4.874
367.50	5.529
466.88	6.100
566.25	6.498
665.63	7.105
766.88	7.438
877.50	7.558
975.00	8.254

Table A7 The amount of methane adsorption (mmol/g) on AC/KOH

Equilibrium pressure (psia)	Methane adsorption (mmol/g)
0.00	0.000
39.38	1.180
71.25	1.827
103.13	2.552
138.75	3.043
176.25	3.495
226.88	3.881
307.50	4.435
412.50	4.917
515.63	5.200
616.88	5.775
727.50	5.831
828.75	5.970
935.63	6.161
1033.13	6.503

Table A8 The amount of methane adsorption ($\mu\text{mol}/\text{m}^2$) on AC/KOH

Equilibrium pressure (psia)	Methane adsorption ($\mu\text{mol}/\text{m}^2$)
0.00	0.000
39.38	1.184
71.25	1.834
103.13	2.561
138.75	3.054
176.25	3.508
226.88	3.896
307.50	4.451
412.50	4.935
515.63	5.219
616.88	5.796
727.50	5.853
828.75	5.991
935.63	6.183
1033.13	6.527

Table A9 The amount of methane adsorption (mmol/g) on AC/NH₃·H₂O

Equilibrium pressure (psia)	Methane adsorption (mmol/g)
0.00	0.000
35.64	0.991
63.76	1.743
93.76	2.325
125.64	2.807
161.26	3.139
198.76	3.886
240.01	4.250
301.89	4.538
395.64	4.889
513.76	5.198
626.26	5.562
729.39	5.753
817.51	6.508
926.26	6.846
1025.64	7.071

Table A10 The amount of methane adsorption ($\mu\text{mol}/\text{m}^2$) on $\text{AC}/\text{NH}_3\cdot\text{H}_2\text{O}$

Equilibrium pressure (psia)	Methane adsorption ($\mu\text{mol}/\text{m}^2$)
0.00	0.000
35.64	1.087
63.76	1.911
93.76	2.549
125.64	3.077
161.26	3.442
198.76	4.260
240.01	4.659
301.89	4.975
395.64	5.359
513.76	5.699
626.26	6.098
729.39	6.307
817.51	7.135
926.26	7.505
1025.64	7.752

Table A11 The amount of methane adsorption (mmol/g) on AC/H₂SO₄

Equilibrium pressure (psia)	Methane adsorption (mmol/g)
0.00	0.000
35.63	0.887
71.25	1.692
101.25	2.243
133.13	2.688
165.00	3.137
206.25	3.459
253.13	3.818
315.00	4.321
406.88	4.857
515.63	5.209
628.13	5.581
729.38	5.836
825.00	6.106
931.88	6.155
1027.50	6.476

Table A12 The amount of methane adsorption ($\mu\text{mol}/\text{m}^2$) on AC/ H_2SO_4

Equilibrium pressure (psia)	Methane adsorption ($\mu\text{mol}/\text{m}^2$)
0.00	0.000
35.63	0.846
71.25	1.614
101.25	2.138
133.13	2.563
165.00	2.991
206.25	3.299
253.13	3.641
315.00	4.120
406.88	4.631
515.63	4.967
628.13	5.322
729.38	5.565
825.00	5.823
931.88	5.869
1027.50	6.175

Table A13 The amount of methane adsorption (mmol/g) on AC/H₂O₂

Equilibrium pressure (psia)	Methane adsorption (mmol/g)
0.00	0.000
39.38	1.257
76.88	2.117
114.38	2.640
146.25	3.054
195.00	3.486
271.88	4.111
367.50	4.614
466.88	5.034
564.38	5.340
663.75	5.706
772.50	5.849
870.00	6.155
986.25	6.776

Table A14 The amount of methane adsorption ($\mu\text{mol}/\text{m}^2$) on AC/H₂O₂

Equilibrium pressure (psia)	Methane adsorption ($\mu\text{mol}/\text{m}^2$)
0.00	0.000
39.38	1.302
76.88	2.192
114.38	2.734
146.25	3.162
195.00	3.610
271.88	4.258
367.50	4.779
466.88	5.213
564.38	5.530
663.75	5.909
772.50	6.057
870.00	6.374
986.25	7.017

Appendix B Ash Content of Activated Carbon on Original and Deashed Activated Carbon**Table B1** Ash Content of Activated Carbon

Activated carbon treatment	% Ash
original	14.15
5% HCl at room temperature for 5 h.	13.33
5% HCl at 60 °C for 5 h.	12.18
15% HCl at room temperature for 5 h.	11.21
15% HCl at room temperature for 25 h.	12.02
HCl+ HF at 70 °C for 5 h.	0.27

Appendix C The Relationship Between the Methane Adsorption Capacity and BET Surface Area from Previous Studies

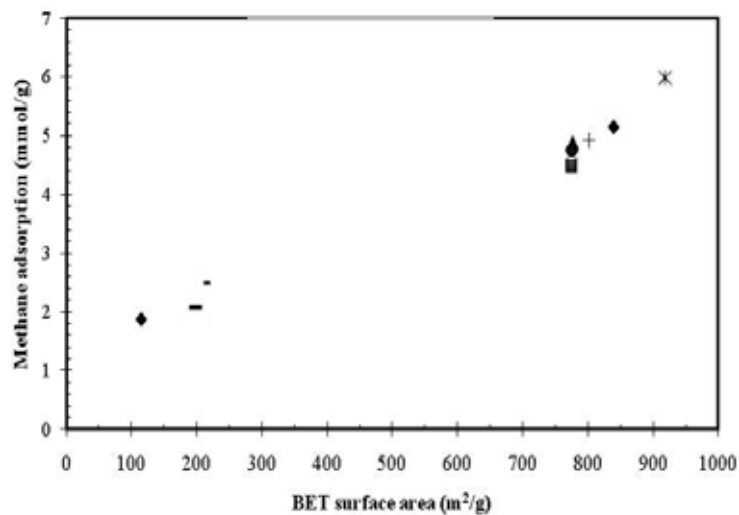


Figure C1 Methane adsorption capacity (mmol/g) at 1000 psia and 40 °C as a function of BET surface area (m²/g) (Sunthonsuriyawong, 2013).

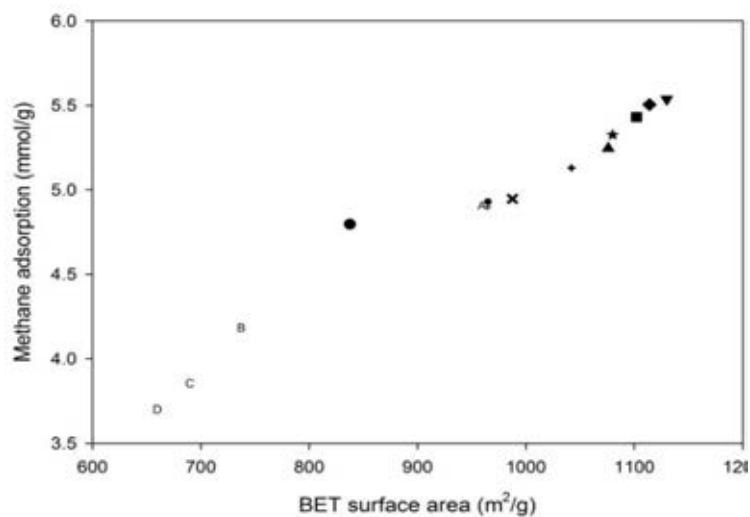


Figure C2 Methane adsorption capacity (mmol/g) at 900 psia and 35 °C as a function of BET surface area (m²/g) (Seangnak, 2014).

